

ABSTRACT OF THE DISSERTATION

HOLOGRAPHIC PROCESSES REALIZABLE IN THE NEURAL REALM:  
PREDICTION OF SHORT TERM MEMORY PERFORMANCE.

J. Patrick Cavanagh

Doctor of Philosophy in Psychology

Carnegie-Mellon University, Pittsburgh, 1972

Professor William G. Chase, Chairman

An associative memory system is proposed based on realizable holographic storage of neural interference patterns. The hypothesis that neural wavefronts represent symbolic information in the brain allows the prediction of behavioural results based on the properties of individual neurons. Among other things, the system predicts Sternberg's (1966) finding of a linear relation between the size of a memorized list and the time required to classify a test item as a member of the list.

Because of the structural coherence of the fixed interneural connections in the brain and the linearity of the neuron as a transducer of mean spike rates, holographic storage is possible under conditions of variable spike train pulse frequencies and random variation in interspike intervals. A matrix analysis of the storage and retrieval of discrete neural wavefronts is presented for two codes commonly found in the brain: frequency or mean rate modulation and steady state mean rate change. Both codes support holographic processes and the expressions for the transmission coefficients of the storage field are developed. Noise and distortion effects in the system are investigated and the ability

to superimpose many interference patterns while still allowing retrieval of individual wavefronts is demonstrated.

A short term memory system is postulated that stores the interference patterns between the wavefront of sensory information received from a stimulus and the wavefront that codes the internal information or "meaning" of the same stimulus. This arrangement allows rapid access recognition of sensory events and imaging of internal symbols.

Since a test stimulus whose appropriate interference pattern has been stored generates a reconstruction of its internal representation while a test stimulus with no stored pattern does not, the system can classify stimuli as positive (stored) or negative (not stored) by monitoring output to the reconstruction area. The amplitude of the reconstructed wavefront depends on the transmission efficiency of the storage field which was found from neurological and mathematical derivations to be exponentially related to  $N$ , the number of items stored in memory. Variation in the time required to detect a wavefront as a function of its amplitude thus predicts reaction time (RT) variation as a function of  $N$ . Both the additive effect of noise on reaction time (Sternberg, 1967) and the relation between simple RT and stimulus intensity lead independently to the conclusion of a logarithmic detection function. The combination of the logarithmic detection-time vs. amplitude relation and the exponential amplitude vs.  $N$  relation predicts that reaction time is a linear function of the number of items memorized and that the slope of the function is the same for positive and negative responses with positives being uniformly faster than negatives. The assumption that the brain optimizes its

processing capacity permits the slope of the RT function to be expressed in terms of the memory span for the type of material being tested. Data from the memory span and memory search literature is shown to support the predicted relation.

The explicit treatment of storage, coding and retrieval parameters in the reaction time expressions derived for the system allows the analysis of many other features of processing on levels ranging from the individual neuron to consciousness itself.

## Table of Contents

Frontispiece.....	ii
Abstract of the dissertation.....	iii
Holographic processes realizable in the neural	
realm: An analysis of short term memory recognition RT.....	1
Optical holography.....	2
Neural holographic processes.....	5
Linear codes.....	5
Neural representation of symbolic information.....	8
Models of neuronal change.....	11
Reconstruction.....	18
MRM code.....	18
DRC code.....	20
The effect of variable amplitude moduli.....	22
Storage of more than one interference pattern.....	24
Evaluation.....	26
Behavioural tasks.....	27
Short term memory recognition.....	27
The item recognition task.....	29
Reaction time predictions of the neural holographic model....	30
Detection functions.....	31
Transmission coefficients.....	33
Reaction time.....	34
Optimization.....	35

Simple reaction time with variable stimulus intensity.....	37
Continuous recognition, perceptual phenomena, and serial position.....	40
Conclusions.....	42
References.....	45
Footnotes.....	51
Figure captions.....	54
Figures.....	57
Appendix A: Constant ratio transmi-sion coefficients.....	64
Appendix B: Optimization of detection.....	68
Appendix C: Data relating memory span to RT function slope.....	70
Appendix D: Latent period vs. intensity.....	71
Appendix E: Simple RT vs. intensity- data.....	72

HOLOGRAPHIC PROCESSES REALIZABLE IN THE NEURAL REALM:

PREDICTION OF SHORT TERM MEMORY PERFORMANCE.<sup>1</sup>

J. Patrick Cavanagh<sup>2</sup>

Carnegie-Mellon University

Holography refers to a broad class of storage and retrieval processes based on the recording of interference patterns. As a model for a neural memory system, holography provides both associative and redundant storage along with a mathematically explicit description of the system's operation. Lashley, in 1929, was among the first to propose that memory was coded in terms of neural interference patterns and was led to this conclusion by his discovery of redundant storage in the brain. Twenty-seven years later, Beurle (1956) showed how such interference patterns might be stored so that the original information could be retrieved without distortion. In 1963, van Heerden noted the similarity between Beurle's hypothesis and the more concise representation of the interference process offered by holographic theory. Subsequently, a number of authors have outlined, to varying degrees, the analogy between holographic and neural processes (Julesz & Pennington, 1965; Pribram, 1966, 1969, 1971; Westlake, 1967, 1968, 1970). Of these, only Westlake (1968, 1970) has given a detailed analysis of the neural mechanisms involved. His hypothesis, however, like Beurle's, places severe restrictions on the firing patterns of neurons that are at odds with the known properties of neural codes.

This dissertation will demonstrate that holographic storage can be obtained when only the most general neural codes are assumed. A recognition system employing transmission holography is proposed and the limited capacity of this type of storage for multiple recordings leads naturally to a modelling of short term memory. The system predicts a wide range of behavioural data in recognition tasks based on a single assumption concerning the properties of individual neurons.

Before detailing the neural holographic processes, a brief description of optical holography will demonstrate some of the properties of this method of storage.

### Optical Holography

Optical holography, developed by Gabor (1948), allows the recording of both the phase and amplitude of a wavefront of light. Since photographic plates are sensitive to intensity but not to phase, the plate is exposed to two wavefronts simultaneously and the resulting interference pattern is recorded. If both wavefronts are monochromatic and coherent in phase, a stable interaction occurs so that the interference pattern codes both amplitude and phase in terms of intensity variations. The recorded interference pattern is the hologram; illuminating the hologram with one of the original wavefronts causes the reconstruction of the other. The hologram is thus an associative memory of the two wavefronts.

If one of the original wavefronts was the light reflected from a three dimensional object, for example, the reconstruction will be an exact replica of the object such that no visual test can differentiate the two. In other words, all of the phase and amplitude information has been recovered.

### Neural representation of symbolic information

The two codes described above characterize single spike trains. A neural wavefront is simply a spatial array of spike trains and will be considered the mode of representation for symbolic information in the brain (stimulus patterns, concepts, motor commands, etc.).

Figure 2 depicts a possible structure for a neural holographic system.  $\underline{a}$  and  $\underline{b}$  are input wavefronts that map through transforms  $X$  and  $Y$ , respectively, onto the storage field neurons.  $\tau$  is the diagonal matrix of transmission coefficients expressing the linear relation between the algebraic sum of the inputs to each neuron and the mean output rate of each neuron--i.e.  $\tau$  represents the efficiency with which input rate variations affect output rate variations.  $W$  and  $Z$  map this output  $\underline{c}$  onto  $\underline{u}$  and  $\underline{v}$ . The transforms  $X, Y, W$ , and  $Z$  are such that with no information recorded in the storage area,  $\underline{a}$  and  $\underline{b}$  are able to cross through each other and end up separately in  $\underline{u}$  and  $\underline{v}$ , respectively.  $\underline{a}$ , in other words, produces no output in  $\underline{v}$  and  $\underline{b}$  no output in  $\underline{u}$ . Simultaneously exposing the storage field to  $\underline{a}$  and  $\underline{b}$  alters the transmission coefficients of these neurons in proportion to the interference pattern of  $\underline{a}$  and  $\underline{b}$ . The spatial variations of  $\tau$  which code this interference pattern now allow wavefront  $\underline{a}$  to produce output in  $\underline{v}$  which, it will be shown, is a reconstruction of  $\underline{b}$ 's output to  $\underline{v}$ . Similarly,  $\underline{b}$  can reconstruct  $\underline{a}$ 's output to  $\underline{u}$ . Thus, the spatial variations of  $\tau$  are the neural hologram.

-----  
 insert Figure 2

about here  
 -----



Expressing these relations mathematically:

$$\underline{u} = W\underline{c} \quad (6)$$

$$\underline{v} = Z\underline{c} \quad (7)$$

$$\underline{c} = \underline{r}_c + \tau(\underline{Xa} + \underline{Yb}) \quad (8)$$

$$\underline{A} = \underline{Xa} \quad (9)$$

$$\underline{B} = \underline{Yb} \quad (10)$$

- denotes that the elements of the variable are coded spike trains  
 $\underline{a}, \underline{b}$  - input wavefronts (column vectors) of discrete pulse trains  
 $\underline{u}, \underline{v}$  - wavefronts arriving at the two output fields (column vectors)  
 $\underline{c}$  - wavefront output from the storage field neurons (column vector)  
 $W, X, Y, Z$  - transform matrices of synaptic coupling coefficients  
 $\underline{A}, \underline{B}$  - the input wavefronts at the storage field (column vectors)  
 $\underline{r}_c$  - column vector of the base firing rates of the storage field neurons  
 $\tau$  - diagonal matrix of transmission coefficients of storage field neurons

Initially  $\tau$  is a scalar matrix (although this is not a necessary assumption, it simplifies analysis).

$$\tau = \lambda I$$

$$\underline{u} = W\underline{r}_c + W\tau(\underline{Xa} + \underline{Yb}) = W\underline{r}_c + W\lambda I\underline{Xa} + W\lambda I\underline{Yb}$$

$$\underline{u} = W\underline{r}_c + \lambda(W\underline{Xa} + W\underline{Yb}) \quad (11)$$

similarly,

$$\underline{v} = Z\underline{r}_c + \lambda(Z\underline{Xa} + Z\underline{Yb}) \quad (12)$$

For  $\underline{a}$  to produce output only in  $\underline{u}$  and  $\underline{b}$  only in  $\underline{v}$ ,

$$WY = 0 \quad ZX = 0 \quad (13)$$

After recording, the transmission coefficients have been altered in some manner. These  $\Delta\tau$ 's are variable across the storage field. For reconstruction,

$\underline{a}$  is again input, but  $\underline{b}$  is zero (ignoring base rates).

$$\begin{aligned}\underline{v} &= Z\tau X_a = Z(\bar{\tau}I + \Delta\tau)X_a & (14) \\ &= Z\bar{\tau}IX_a + Z\Delta\tau X_a & \bar{\tau} - \text{average value of } \tau \\ &= \bar{\tau}ZX_a + Z\Delta\tau X_a & \Delta\tau - \text{diagonal matrix of variations of} \\ & & \tau \text{ around } \bar{\tau}\end{aligned}$$

$$ZX = 0$$

$$\underline{v} = Z\Delta\tau X_a \quad (15)$$

Any term in  $\tau$ , therefore, that is constant over all storage neurons does not generate any output in the reconstruction field. Thus,  $\Delta\tau X_a$  must contain  $\underline{Y}_b$  (i.e.  $\Delta\tau A$  must contain  $\underline{B}$ ) if an accurate reconstruction is to be produced.

The relations between  $W$  and  $Y$  and  $Z$  and  $X$  expressed in equation 13 are essential to the processing of the neural wavefronts and are analogous to the recording geometries in optical holography that allow separation of output images. It is possible, because of their importance to processing, that these relations have developed through evolution; conversely,  $\underline{u}$  and  $\underline{v}$  may simply be the subset of output fields of the storage neurons whose transforms obey these relations.

The feedback loops shown in Figure 2 illustrate that this structure could be two circulating neural nets that intersect at a set of modifiable neurons. The association between the various "cell assemblies" (Hebb, 1949) realizable in the nets thus occurs at their intersection.

Finally, in analyzing storage and reconstruction, only the wavefronts at the storage field,  $\underline{A}$  and  $\underline{B}$ , need be considered as these are the wavefronts that directly produce the interference pattern to be stored. The expressions for  $\underline{A}$  and  $\underline{B}$  are, for MRM coding where the subscript  $i$  indicates input activity at the  $i^{\text{th}}$  storage neuron are

$$\underline{A} = \underline{X}_a = [r_{A_i} + A_i \cos(2\pi ft + \theta_i)] \quad (16)$$

$$\underline{B} = \underline{Y}_b = [r_{B_i} + B_i \cos(2\pi ft + \phi_i)] \quad (17)$$

and for DRC coding,

$$\underline{A} = \underline{X}_a = [r_{A_i} + A_i \text{evn}\theta_i] \quad (18)$$

$$\underline{B} = \underline{Y}_b = [r_{B_i} + B_i \text{evn}\phi_i] \quad (19)$$

### Models of neuronal change

At present, the basis of neuronal change is unknown, but there are a number of hypotheses of the factors that might lead to such change (Kupfermann & Pinsker, 1969) and these fall into two main classes. The first states that the degree of usage of the synaptic terminals or of the postsynaptic cell somehow affects their subsequent efficiency. The second proposes that the concurrence of action potentials at the pre- and postsynaptic membranes and the consequent permeability of both, allows some form of molecular communication that effects a change in transmission efficiency; the probability of concurrence at each synapse will depend both on the output rate of the postsynaptic cell and on the input rate at the synapse.

To allow holographic storage, the neuronal change must code the linear interaction of the two inputs  $\underline{A}$  and  $\underline{B}$  (i.e.  $\underline{A+B}$ ). This requirement is met by the postsynaptic use and concurrent use hypotheses, both of which reflect the output rate ( $\underline{A+B}$ ) of the postsynaptic cell; the synaptic use hypothesis, however, reflects only the input to each particular synapse and so cannot support holographic processes. Furthermore, since the inhibitory and excitatory components of an input cancel in their effect on the output of the postsynaptic cell, isomorphic coding requires that their effects on the transmission efficiency of a cell

also cancel. This is satisfied by the postsynaptic use hypothesis (simple use) where neuronal change is a function only of the output rate of the postsynaptic cell. In the case of concurrent use, the agent of neuronal change is the substance passing between pre- and postsynaptic processes and this interchange is a function not only of postsynaptic firing but also of the input rates at each synapse. For the molecular agents of inhibitory and excitatory inputs to counteract each other, they must be mutually antagonistic and must be able to diffuse and interact, even if only on a local basis (assuming random spatial distribution of inputs), after passing across the postsynaptic membrane. If input to each cell is either all inhibitory or all excitatory, this cancellation requirement is, of course, unnecessary and the transport can be in either direction across the synaptic cleft (this form of the concurrence hypothesis is typically called specific use).

Finally, it can be shown that when the function expressing neuronal change (the transmission function) contains linear terms in  $A$  or  $B$ , significant noise results in the reconstruction field. Since MRM coding is periodic, any linear terms will average to zero over one period; DRC coding, however, is not time varying and linear terms can only be suppressed in the concurrence hypotheses with certain restrictions and cannot be suppressed at all in the simple use case (requiring, therefore, the absence of linear terms, and, in fact, all odd-powered terms, in the transmission function).

To summarize the properties of the various hypotheses: holographic storage of MRM coded input is supported by simple and concurrent use and by specific use when input to each cell is either all excitatory or inhibitory; holographic storage of DRC coded input is possible for special cases of simple and specific use; the change in neuronal

transmission efficiency ( $\tau$ ) involves the cell as a unit in simple use, local areas of the cell in concurrent use (in both cases, the change affects all input to the cell equally), and individual synapses in specific use.

The neural holographic process will be analyzed for the case of concurrent use where each concurrence contributes equally to the change in transmission efficiency. Although any number of other models could have been chosen for analysis, this particular model has a number of advantages: it offers more structure and fewer restrictions than the simple use model; it applies equally to processing units of single cells or ensembles of cells; the equality of the effect of each concurrence is intuitively attractive; the results generalize readily to the specific use model; and behavioural data discussed in the latter half of this paper show that the transmission function must be an exponential (see Appendix A) and such a function is a fundamental characteristic of the model to be considered.

The selected model postulates that concurrent use leads to change, but change in what direction? Most experimental evidence, especially in the peripheral nervous system, suggest that use weakens, rather than strengthens, the transmission efficiency of a cell when input is excitatory (Sharpless, 1964). Such a change is compatible with the phenomena of habituation, extinction, and spontaneous recovery, among others. Griffiths (1966) has demonstrated how this weakening acts as negative feedback to stabilize neuron output; if, conversely, use led to strengthening, the concomitant positive feedback would produce instability or runaway in the cell's output.

No experimental work has been done on the effects of inhibitory

input. However, to obtain the same stability, concurrence of the post-synaptic action potential with the arrival of inhibitory impulses must lead to strengthening of the effectiveness of inhibitory input. If weakening (i.e. release from inhibition) were to result, the cell's output would again increase autonomously.

The concurrence of action potentials at a synapse must affect not only the synapse involved but also neighbouring synapses which may be of similar or different nature. This can be accomplished if the molecular agent released by an inhibitory concurrence strengthens, and that released by an excitatory concurrence weakens, the receptor sensitivity of either type of synapse. These two actions are then also mutually antagonistic, as previously required. Since the model is addressing short term memory processes with a time scale in the order of seconds, such changes in receptor sensitivity (assuming excitatory input) might be seen on a gross level as fatigue or accommodation, a consistently observable cellular phenomenon.

Various assumptions have been made concerning the mechanisms of neuronal change and the analysis of holographic storage and retrieval will now be undertaken based on these assumptions. It must be emphasized that the feasibility of holographic processes does not depend on these assumptions and that equivalent derivations result from a variety of other neuronal models.

Figure 3 shows a single neuron (chosen arbitrarily so that no subscripts will be used) where A represents the algebraic sum of input from the a wavefront and B the sum from the b wavefront.

-----  
 insert Figure 3 about here  
 -----

Considering the MRM code, when the total synaptic effect is positive. then the output of the cell is in phase with the input. With multisynaptic

input, the input and output processes can be considered independent<sup>4</sup> with linearly related means. The expected number of concurrent pre- and postsynaptic action potentials (hits) per unit time is then directly proportional to the product of the mean input and output rates.

$$E(\text{hit}) = E\{(r_C + \tau(\underline{A} + \underline{B})) \cdot (\underline{A} + \underline{B})\} \quad (20)$$

E - expected value

Assuming that the duration of exposure,  $\tau$ , is a random variable unrelated to the period of the modulating wavefront, the expected number of hits can be estimated by averaging over one period,

$$E(\text{hit}) = \frac{1}{2\pi} \int_0^{2\pi} (r_C + \tau(r_A + r_B + A \cos(2\pi f t + \theta) + B \cos(2\pi f t + \phi))) \cdot (r_A + r_B + A \cos(2\pi f t + \theta) + B \cos(2\pi f t + \phi)) d(2\pi f t)$$

$$E(\text{hit}) = \tau(r_A + r_B)^2 + r_C(r_A + r_B) + \tau(A^2 + B^2 + 2AB \cos \gamma) \quad (21)$$

where  $\gamma = \theta - \phi$

$\gamma$  - the phase difference between the two inputs

If each hit contributes an equal amount to the weakening of the transmission efficiency, then the rate of change of  $\tau$  will be linearly related to  $E(\text{hit})$ . Assuming an equilibrium process that maintains  $\tau$  at a steady level when there is no input other than the base rates, the expression is,

$$\begin{aligned} \frac{d\tau}{dt} &= -\alpha E(\text{hit}) + \alpha(\tau(r_A + r_B)^2 + r_C(r_A + r_B)) \\ &= -\alpha\tau(A^2 + B^2 + 2AB \cos \gamma) \end{aligned} \quad (22)$$

Integrating over  $\tau$ , the total time for which the storage neuron is exposed to  $\underline{A}$  and  $\underline{B}$ ,

$$\tau = \lambda e^{-\alpha\tau(A^2 + B^2 + 2AB \cos \gamma)} \quad (23)$$

$\alpha, \lambda$  - constants

If the total synaptic effect is inhibitory, the output  $\underline{c}$  will decrease when input  $(\underline{A+B})$  increases. Therefore

$$E(\text{hit}) = E\{(r_c - \tau(\underline{A+B})) \cdot (\underline{A+B})\} \quad (24)$$

and the average, as in equation 21, over one period is,

$$E(\text{hit}) = -\tau(r_A + r_B)^2 + r_c(r_A + r_B) - \tau(A^2 + B^2 + 2AB\cos\gamma) \quad (25)$$

However, each hit now contributes to the increase of  $\tau$ . Again, with an equilibrium process,

$$\begin{aligned} \frac{d\tau}{dt} &= +\alpha E(\text{hit}) + \alpha(\tau(r_A + r_B) - r_c(r_A + r_B)) \\ &= -\alpha\tau(A^2 + B^2 + 2AB\cos\gamma) \\ &\quad -\alpha\tau(A^2 + B^2 + 2AB\cos\gamma) \end{aligned}$$

again  $\tau = \lambda e$

As expected, both excitatory and inhibitory input (and therefore any combination of the two) lead to the same storage characteristic.  $\alpha$  represents the storage parameter, the strength with which incoming information alters the cell.  $\lambda$  is simply the base level of  $\tau$  with no information stored and  $t$  represents the exposure time of the input. The elements of  $[\tau]$ , the diagonal matrix of transmission coefficients that codes the neural hologram, are given by

$$\tau_{ii} = \lambda e^{-\alpha t(A_i^2 + B_i^2 + 2A_i B_i \cos\gamma_i)}$$

For the DRC code, there are limitations on the interneural connections and base firing rates that will allow useful storage. The restrictions are that the total synaptic effect must be inhibitory and that the base rates are related as follows

$$r_c = 2(r_A + r_B) \quad (26)$$

In electrical engineering terms, equation 26 places the quiescent point midway in the operating range of the neuron. It is the optimum



operating point in that it allows the maximum signal input without distortion; nevertheless, it is a definite restriction on the generality of the model. The expected rate of hits in this case is,

$$E(\text{hit}) = -\tau(r_A+r_B)^2 + r_C(r_A+r_B) + (r_C-2\tau(r_A+r_B)) \cdot (A\text{evn}\theta+B\text{evn}\phi) - \tau(A\text{evn}\theta+B\text{evn}\phi)^2$$

Because of the restriction of equation 26, this reduces to

$$E(\text{hit}) = -\tau(r_A+r_B)^2 + r_C(r_A+r_B) - \tau(A\text{evn}\theta+B\text{evn}\phi)^2 \quad (27)$$

Thus the combined effect of the two restrictions is to eliminate the first order terms of  $\text{evn}\theta$  and  $\text{evn}\phi$ . It can be shown that these terms make any useful reconstruction of information impossible.

The rate of change of  $\tau$  is now,

$$\begin{aligned} \frac{d\tau}{dt} &= \alpha E(\text{hit}) + \alpha(\tau(r_A+r_B)^2 - r_C(r_A+r_B)) \\ &= -\alpha\tau(A\text{evn}\theta+B\text{evn}\phi)^2 \end{aligned}$$

since  $(\text{evn}\theta)^2$ ,  $(\text{evn}\phi)^2 = 1$

and  $\text{evn}\theta \cdot \text{evn}\phi = \text{evn}(\theta-\phi)$

$$\frac{d\tau}{dt} = -\alpha\tau(A^2+B^2+2AB\text{evn}\gamma) \quad (28)$$

where  $\gamma = \theta - \phi$

$$\text{thus } \tau = \lambda e^{-\alpha t(A^2+B^2+2AB\text{evn}\gamma)} \quad (29)$$

$$\text{and } \tau_{ij} = \lambda e^{-\alpha t(A_i^2+B_i^2+2A_i B_i \text{evn}\gamma_i)}$$

Both codes have led to the conclusion of an exponential storage characteristic. That is, the transmission coefficients of the neurons which encode the interference pattern of the two wavefronts vary exponentially with the input signals. It has been shown optically (Friesem & Zelenka, 1967) that reconstruction is possible with nonlinear recording characteristics. The main effect of the nonlinearity is to

produce higher order images analogous to the higher order diffractions from an optical grating. These unwanted images can typically be separated from the desired reconstruction.

At present no analysis of the possibility of decay of stored information will be made, as it does not play an important role in the behavioural tasks to which the model will be applied. The mechanism of storage implies that there may be an exponential decay although this is not strictly true. The information might remain unchanged over time until some external control signal effectively caused it to be erased. In a similar manner, a control signal might also govern the recording of information, increasing the value of  $\alpha$  (equations 23 and 29) to store interference patterns and decreasing  $\alpha$  to ignore them.

### Reconstruction

Having developed expressions for  $\tau$ , the form of the reconstructed wavefront can now be determined. Initially, the amplitude moduli,  $A$  and  $B$ , will be assumed constant for each neuron to simplify the derived expressions; the effect of relaxing this assumption is analyzed at the end of this section.

To obtain reconstruction after the interference pattern of  $\underline{A}$  and  $\underline{B}$  has been stored,  $\underline{A}$  alone or  $\underline{B}$  alone is input to the storage field.

MRM code. Considering reconstruction with the input of the  $\underline{A}$  wavefront, output at an arbitrary neuron is,

$$\underline{c} = r_c + \lambda e^{-\alpha t(A^2+B^2+2AB\cos\gamma)} \cdot (r_A+r_B+A\cos(2\pi ft+\theta)) \quad (30)$$

As demonstrated by Tokarski (1968) in the optical case, the transmission coefficient can be expanded in a Fourier cosine series to determine

the image producing term,

$$\underline{c} = r_c + (r_A + r_B + A \cos(2\pi f t + \theta)) \cdot \left( \lambda \sum_0^{\infty} T_m \cos(m\gamma) \right) \quad (31)$$

$T_m, m=0,1,2,\dots$  - Fourier coefficients

Only the term for  $m=1$  will contain a replica of the  $\underline{B}$  wavefront, all terms for  $m>1$  produce higher order images. The  $m=0$  term is a constant.

The first two Fourier coefficients are,

$$\begin{aligned} T_0 &= \frac{1}{2\pi} \int_0^{2\pi} e^{-\alpha t(A^2+B^2+2AB\cos\gamma)} d\gamma \\ &= e^{-\alpha t(A^2+B^2)} \cdot I_0(2\alpha tAB) \end{aligned} \quad (32)$$

$I_0$  - zero order modified Bessel function

$$\begin{aligned} T_1 &= \frac{1}{\pi} \int_0^{2\pi} e^{-\alpha t(A^2+B^2+2AB\cos\gamma)} \cdot \cos\gamma d\gamma \\ &= -2e^{-\alpha t(A^2+B^2)} \cdot I_1(2\alpha tAB) \end{aligned} \quad (33)$$

$I_1$  - first order modified Bessel function

$$\begin{aligned} \text{thus } \underline{c} &= r_c + (r_A + r_B) \lambda \left( \sum_0^{\infty} T_m \cos(m\gamma) \right) + A \cos(2\pi f t + \theta) \lambda e^{-\alpha t(A^2+B^2)} I_0(2\alpha tAB) \\ &\quad - A \cos(2\pi f t + \theta) \left( 2\lambda e^{-\alpha t(A^2+B^2)} \cdot I_1(2\alpha tAB) \right) \cos\gamma \\ &\quad + \text{higher order terms} \end{aligned} \quad (34)$$

In equation 34:  $r_c$  will produce the base firing rates at the output field;  $r_A + r_B$  and  $\cos m\gamma$  are independent and so will generate a randomly distributed noise field that is subsumed in the base rates at  $\underline{v}$ ; the third term is constant for all the neurons of the storage field so that there is no output in  $\underline{v}$  as a result of this term (equations 14 and 15); the fourth term is the reconstruction term; the higher order terms propagate to  $\underline{v}$ , but, analogous to the optical case, can be separated from the desired

reconstruction by the transform  $Z$ . The reconstruction term is then,

$$c_r = -\lambda A e^{-\alpha t(A^2+B^2)} I_1(2\alpha tAB) (2\cos(2\pi ft+\theta) \cdot \cos\gamma)$$

but  $\gamma = \theta - \phi$

$$c_r = -\lambda A e^{-\alpha t(A^2+B^2)} I_1(2\alpha tAB) (\cos(2\pi ft+\phi) + \cos(2\pi ft+2\theta-\phi)) \quad (35)$$

Since amplitude moduli were assumed constant, only the phase of the  $\underline{B}$  wavefront need be recovered for reconstruction. This is the case in equation 35, the first cosine term being the phase of  $\underline{B}$ . The leading terms represent the amplitude of the  $\underline{B}$  reconstruction; the second cosine term is the complement of  $\underline{B}$  and is similar to the conjugate image in optical holography.

Thus a linear reconstruction of the  $\underline{B}$  wavefront has been obtained (the linearity is partially a result of the assumption of constant amplitude moduli) allowing the conclusion that neural holography can be achieved using this very general mean rate modulation code. The complementary and higher order reconstructions are equivalent to the multiple images produced in optical holography. It is reasonable to assume that these can be separated from the desired reconstruction given the appropriate anatomy of the neural structure.

DRC code. The analysis of reconstruction with the DRC code leads to a rather significant result. Considering again input of the  $\underline{A}$  wavefront alone, equations 8 and 29 give

$$\underline{c} = r_c - (r_A + r_B + A e^{v n \theta}) \lambda e^{-\alpha t(A^2+B^2+2ABevn\gamma)}$$

Expanding the variable part of the exponential,

$$\underline{c} = r_c - (r_A + r_B + A e^{v n \theta}) \lambda e^{-\alpha t(A^2+B^2)} \cdot \left\{ 1 - 2\alpha tABevn\gamma + \frac{(2\alpha tABevn\gamma)^2}{2!} - \dots \right\}$$

but  $(evn\gamma)^{2n} = 1$

and  $(\text{evn}\gamma)^{2n+1} = \text{evn}\gamma$   $n$  - any integer

$$\begin{aligned} \underline{c} &= r_c - (r_A + r_B + A\text{evn}\theta)\lambda e^{-\alpha t(A^2+B^2)} \cdot \left\{ 1 + \frac{(2\alpha tAB)^2}{2!} + \frac{(2\alpha tAB)^4}{4!} + \dots \right. \\ &\quad \left. - (2\alpha tAB)\text{evn}\gamma - \frac{(2\alpha tAB)^3\text{evn}\gamma}{3!} - \frac{(2\alpha tAB)^5\text{evn}\gamma}{5!} - \dots \right\} \\ \underline{c} &= r_c - (r_A + r_B + A\text{evn}\theta)\lambda e^{-\alpha t(A^2+B^2)} \cdot \left\{ \cosh(2\alpha tAB) - \sinh(2\alpha tAB)\text{evn}\gamma \right\} \quad (36) \\ \underline{c} &= r_c - (r_A + r_B + A\text{evn}\theta)\lambda e^{-\alpha t(A^2+B^2)} \cosh(2\alpha tAB) \\ &\quad + (r_A + r_B)\lambda e^{-\alpha t(A^2+B^2)} \sinh(2\alpha tAB)\text{evn}\gamma \\ &\quad + \lambda A e^{-\alpha t(A^2+B^2)} \sinh(2\alpha tAB)\text{evn}\theta\text{evn}\gamma \quad (37) \end{aligned}$$

$r_c$  is again the base rate; the second term contains the direct transmission coefficient which is constant for all neurons and therefore allows propagation to  $\underline{u}$  but not to  $\underline{v}$ ; in the third term  $r_A + r_B$  and  $\text{evn}\gamma$  are independent variables and thus produce randomly distributed noise in  $\underline{v}$ ; the fourth term is the reconstruction term.

$$c_r = \lambda A e^{-\alpha t(A^2+B^2)} \sinh(2\alpha tAB)\text{evn}\theta\text{evn}\gamma$$

but  $\text{evn}\theta \cdot \text{evn}\gamma = \text{evn}(\theta - \gamma)$

and  $\gamma = \theta - \phi$

$$c_r = \lambda A e^{-\alpha t(A^2+B^2)} \sinh(2\alpha tAB) \cdot \text{evn}\phi \quad (38)$$

The direction dimension of the  $\underline{B}$  wavefront is recovered ( $\text{evn}\phi$ ) and since amplitude moduli were assumed constant,  $\underline{B}$  has been linearly reconstructed. The important result is that only one wavefront component is generated; the complement of  $\underline{B}$  is not produced nor are higher order images even though the recording is nonlinear (this result will hold for any form of nonlinearity). This simplicity in the output space, which cannot be obtained in the optical or neural MRM cases, permits a great deal

of generality in the neural anatomies appropriate for holographic processes.

The effect of variable amplitude moduli. The previous sections have dealt with storage and reconstruction with the assumption of a constant amplitude of input to each neuron. The information stored and recovered was that of phase or direction. Allowing the amplitude moduli, A and B, to vary over the storage neurons increases the amount of information that can be represented, while still permitting the faithful recovery of phase or direction. It is not possible, however, to recover the amplitude terms without a certain amount of noise and distortion. Since the condition of strictly constant moduli is unlikely in the brain, it is important to determine the form of the resulting distortion.

Examination of equations 34 and 37 shows that there are three sources of distortion. First, the terms  $\{\lambda e^{-\alpha\tau(A^2+B^2)} J_0(2\alpha\tau AB)\}$ , from equation 34, and  $\{\lambda e^{-\alpha\tau(A^2+B^2)} \cosh(2\alpha\tau AB)\}$ , from equation 37, are the direct transmission coefficients. As the constant terms in  $\tau$ , they allow propagation to  $\underline{u}$  but not to  $\underline{v}$ . With variable moduli, these expressions are no longer constants. Their spatial variation is independent of  $\theta$  and  $\phi$  and so produces a uniform noise output to  $\underline{v}$  that increases in proportion to the variance of A and B. The effect of the noise depends on the ratio of the "area" in  $\underline{v}$  to which the  $\underline{B}$  wavefront propagates, to the total "area" reached by the noise. This ratio is determined by the output transform Z which could theoretically shrink the reconstruction "area" to minimize the effect of the noise.

The second source of distortion arises from the encoding of the amplitude in the product of an exponential and a Bessel (equation 34)

or a hyperbolic sine (equation 37) function. To determine if the amplitude of  $\underline{B}$  is recoverable, the products are expanded; from 34

$$\alpha t A \cdot e^{-\alpha t A^2} \cdot \left\{ B - \alpha t \left( 1 - \frac{\alpha t A^2}{2} \right) B^3 + \dots \right\} (\cos \phi + \cos(2\theta - \phi)) \quad (39)$$

and from 37

$$2\alpha t A \cdot e^{-\alpha t A^2} \cdot \left\{ B - \alpha t \left( 1 - \frac{2\alpha t A^2}{3} \right) B^3 + \dots \right\} \text{evn} \phi \quad (40)$$

The expansions do contain first order terms in  $B$ . The first nonlinear term is cubic; however, the coefficient of this term can be made to equal zero with appropriate values of  $\alpha$ ,  $t$ , and  $A$ .

The third source of distortion can be seen in equations 39 and 40. The terms to the left of the braces should be constant for a faithful reconstruction; the value of  $A$ , however, is variable. The variance of  $A$  around its mean value thus superimposes a random field of noise on top of the reconstructed  $\underline{B}$  wavefront. Again there is a tradeoff between the increased information capacity with variable moduli and the resulting increase in noise.

These sources of noise and distortion are similar to those faced in optical holography where a careful choice of recording geometries and techniques usually suffices to minimize their effects. It is evident that if the brain were to use holographic storage, it too would have to make careful choices of neural transforms and signal codes; these choices could be made by natural selection in evolution.

In addition, the brain might have another mechanism to aid in noise suppression. If the neural holographic structure were two intersecting networks as suggested previously, the self-seeking reverberations of such networks could act as feedback to suppress nonlinearities and random variability.

Storage of more than one interference pattern

It is possible for the neural hologram to record more than one interference pattern while still allowing separate retrieval of wavefronts from individual patterns. The equivalent optical case (multiple storage on two dimensional holograms) has been analyzed by Collier and Pennington (1967); their study showed that reconstruction with no crosstalk is possible when the wavefronts being stored are uniquely coded--i.e. their cross-correlations with other wavefronts to be stored are minimal or zero. This result generalizes readily to the neural case as the wavefronts A and B vary uniquely over the storage field and can be assumed to have little correlation to subsequent sets of wavefronts being stored. Collier and Pennington reported that the crosstalk in this case is transformed into uniformly distributed noise that does not impair reconstruction.

Storage of multiple patterns in the neural case is achieved by the sequential exposure of the storage field to pairs of input wavefronts. For the MRM code then,

$$\tau = \lambda e^{-\alpha \sum_{j=1}^N t_j (A_j^2 + B_j^2 + 2A_j B_j \cos \gamma_j)}$$

N - number of patterns stored

Assuming that the wavefronts have the same average amplitude moduli and that exposure times are equal,

$$\tau = \lambda e^{-\alpha N t (A^2 + B^2) - 2\alpha t AB \sum_{j=1}^N \cos \gamma_j}$$

Expanding as the product of N Fourier cosine series (equations 32 and 33),

$$\tau = \lambda e^{-\alpha N t (A^2 + B^2)} \cdot \prod_{j=1}^N \{ I_0(2\alpha t AB) - 2I_1(2\alpha t AB) \cos \gamma_j + \dots \}$$



$$\begin{aligned} \tau = \lambda e^{-\alpha N + (A^2 + B^2)} &\cdot \{I_0(2\alpha AB)\}^N \\ &- 2\lambda e^{-\alpha N + (A^2 + B^2)} \cdot \{I_0(2\alpha AB)\}^{N-1} \cdot \{I_1(2\alpha AB)\} \cdot \sum_{j=1}^N \cos \gamma_j \\ &+ \text{intermodulation and higher order terms} \end{aligned} \quad (41)$$

The first term is the direct transmission coefficient; the second is the reconstruction transmission coefficient--each  $\cos \gamma_j$  contains the information for reconstruction of the  $j^{\text{th}}$  wavefront. Intermodulation or crosstalk is produced, on input of the  $i^{\text{th}}$  wavefront, by the cosine terms for  $j \neq i$  and by the terms containing products of two or more cosines.

Similarly for the DRC code,

$$\tau = \lambda e^{-\alpha N + (A^2 + B^2) - 2\alpha AB \sum_{j=1}^N \epsilon v n \gamma_j}$$

Expanding as a product of  $N$  Taylor series (from equation 36),

$$\begin{aligned} \tau = \lambda e^{-\alpha N + (A^2 + B^2)} &\cdot \prod_{j=1}^N \{ \cosh(2\alpha AB) - \sinh(2\alpha AB) \cdot \epsilon v n \gamma_j \} \\ \tau = \lambda e^{-\alpha N + (A^2 + B^2)} &\cdot \{ \cosh(2\alpha AB) \}^N \\ &- \lambda e^{-\alpha N + (A^2 + B^2)} \cdot \{ \cosh(2\alpha AB) \}^{N-1} \cdot \{ \sinh(2\alpha AB) \} \cdot \sum_{j=1}^N \epsilon v n \gamma_j \\ &+ \text{intermodulation terms} \end{aligned} \quad (42)$$

The terms are equivalent to those for the MRM code.

Notice in equations 41 and 42 that the reconstruction transmission coefficients have the same value for each of the  $N$  patterns. That is, the order of storage does not affect the amplitudes of the reconstructed wavefronts. This lack of a serial position effect would not have resulted if some form of storage decay had been assumed. Notice also that the amplitude of reconstruction decreases exponentially with the number

of patterns stored. This implies that the transmission type neural hologram is a limited capacity store. Phase holography (Upatnieks & Leonard, 1970) does not attenuate amplitude as increasing numbers of patterns are stored and so might be a candidate model for a large capacity storage such as long term memory.

### Evaluation

The neural hologram has been shown to be capable of multiple storage of associations such that information from individual associations can be retrieved. There might be many structures in the brain that are able to support these holographic processes. The configuration of input converging from two different areas is, of course, widespread. In addition, the two codes analyzed are found in many areas of the brain. It is a very difficult task, however, to determine whether the appropriate transforms are available. Thus, while holography is a feasible storage process in the brain, little can be done to test it physiologically.

Nevertheless, the holographic hypothesis can be investigated on the behavioural level. Since expressions have been derived that give the signal strength of reconstructed wavefronts, any behavioural task in which performance depends on this parameter should provide a test of the hypothesis. The next section deals with the short term memory (STM) item recognition task developed by Sternberg (1966) and shows that the neural holographic storage does indeed predict the results of this experiment.

## Behavioural Tasks

Short term memory recognition

Figure 4 illustrates a possible organization for holographic short term memory that has many advantages. The essential feature is that the storage area records the interference pattern of the internal and external representations of a stimulus. In Figure 4, then, the wavefront A codes the sensory information<sup>5</sup> (external label) about the stimulus while B codes the internal representation (meaning) of the same stimulus. This arrangement allows rapid access of the internal representations of current sensory events for cognitive processing. If a sensory event does not have its internal-external association stored in STM, an attempt is made to retrieve the appropriate label from long term memory (LTM) presumably involving a longer delay in retrieval.

The hypothesis also allows internal labels to reconstruct sensory representations, implying that holographic STM can be responsible for imaging processes. As a final and strongly intuitive conjecture, it will be assumed that consciousness (perception or awareness) of a stimulus accompanies the concurrent activity of its appropriate internal and external representations. In other words, when a stimulus is imaged or perceived, both internal information (meaning) and sensory information are simultaneously available. The duration of overlap of internal and external wavefront activity is the storage time,  $t$ , for the stimulus; no overlap infers no storage. The conjecture that concurrence implies consciousness not only presumes that some degree of overlap, and therefore storage, is possible but also proposes that the duration of the overlap is a reportable, and thus perhaps measurable, phenomenological event.

For example, a timed protocol

overt rehearsal could reveal the items stored and their respective total storage times.

The model thus provides an isomorphism between phenomenological and neural events in STM tasks. The particular task to be considered

-----  
 insert Figure 4

about here  
 -----

requires the classification of a test stimulus as stored or not stored. Since presenting a stimulus item that has been stored causes a reconstruction while a stimulus that has not been stored does not, detectors monitoring output to v and to u can classify the stimulus correctly. Figure 5 presents the schematic for this recognition system. The gate signifies that a reconstructed wavefront results only if an interference pattern appropriate to the test stimulus has been stored. A positive response is generated if a wavefront is detected at v; a negative response is generated if the wavefront at u is detected before a detection occurs at v. Since expressions for the transmission coefficients have been derived, the signal strength reaching the detectors is known. If the relation between the detection times,  $t_{dr}$  and  $t_{do}$ , and the strengths of the signals to be detected can be determined, then the reaction time for classification can be predicted.

-----  
 insert Figure 5

about here  
 -----

The next section outlines the procedure and results of the classification task, or as it is more frequently described, item recognition.

### The item recognition task

This paradigm was originally investigated by Sternberg (1966). A subspan list of variable length is memorized at the start of each trial (Sternberg used lists of one to six different digits presented sequentially at a rate of about one digit per second). After a short interval of one or two seconds, a test stimulus is displayed and the subject attempts to classify it as stored (positive response) or not stored (negative response) as rapidly and accurately as possible (error rate is usually less than 5%). The dependent variable is the reaction time from the onset of the test stimulus to the classification response; the independent variable is the number of items memorized.

A typical outcome for this type of experiment is shown in Figure 6.

-----  
insert Figure 6

about here  
-----

There are three important features in these results:

1. The mean reaction time (RT) is linearly related to the number of items memorized for both positive and negative responses.
2. The slopes of the linear relations are equal for positive and negative responses. The value of the slope parameter is in the order of 30 to 40 ms for digits.
3. With equal positive and negative response frequencies, the intercept for positive response latencies is typically about 50 ms less than that for negatives.

This pattern of results has held up over a wide variety of procedural variations (Chase & Calfee, 1968; Clifton & Birenbaum, 1970; Hoving, Morin & Konick, 1970; Burrows & Okada, 1971; Klatzky & Atkinson,

1971) although some studies (Briggs & Swanson, 1968; Yio & Santa, 1971) have reported negatively accelerated RT functions. Finally, mixed results have been obtained concerning the variation of positive reaction times as a function of the position of the test item in the memorized list. No serial position effect was found by Juola and Atkinson (1971), or Cavanagh and Chase (1971). Klatzky and Atkinson (1971), however, reported faster reaction times for items at the beginning of lists (primacy); Clifton and Birenbaum (1970) found fastest reaction time for end items (recency) when delay between memorization and test was less than one second; and Burrows and Okada (1971) reported both primacy and recency.

#### Reaction time predictions of the neural holographic model

From Figure 5, the total reaction time for the positive and negative responses can be expressed as follows

$$RT^+ = t_s + t_H + t_{dr} + t_R$$

$$RT^- = t_s + t_H + t_{do} + t_R$$

- RT<sup>+</sup> - positive reaction time
- RT<sup>-</sup> - negative reaction time
- t<sub>s</sub> - wavefront transmission time from receptors to input field
- t<sub>H</sub> - wavefront transmission time from input field to detectors
- t<sub>dr</sub> - reconstruction wavefront detection time
- t<sub>do</sub> - directly transmitted wavefront detection time
- t<sub>R</sub> - response execution time

The response execution times are assumed equal for equal positive and negative response frequencies. Combining the constant reaction time components and expressing the detection times as functions of the amplitudes of the wavefronts to be detected (omitting base rates and assuming insensitivity to phase or direction terms),

$$RT^+ = t_c + d_r (\tau_r \cdot A \cdot s_r) \quad (43)$$

$$RT^- = t_c + d_o (\tau_o \cdot A \cdot s_o) \quad (44)$$

$t_c$  -- combined constant reaction time components  
 $d_r$  -- reconstruction detection function  
 $d_o$  -- direct transmission detection function  
 $\tau_r$  -- reconstruction transmission coefficient  
 $\tau_o$  -- direct transmission coefficient  
 $A$  -- amplitude of the input  $A$  wavefront  
 $s_r$  -- reconstruction detector sensitivity  
 $s_o$  -- direct transmission detector sensitivity

The sensitivities,  $s_r$  and  $s_o$ , of the two detectors are included to represent the control of attentional processes in achieving various combinations of speed and accuracy.  $A$ , the amplitude of the wavefront representing the stimulus can be assumed constant from trial to trial. Of the terms in equations 43 and 44, only the transmission coefficients are affected by  $N$ , the number of items memorized. Prediction of reaction times thus depends on determining the detection functions,  $d_r$  and  $d_o$ .

Detection functions. Sternberg (1967) and Bracey (1969) have repeated the item recognition task with a visual pattern superimposed on the test item to determine the effects of stimulus degradation on reaction time. Both studies found that the visual noise affected the intercepts of the RT vs.  $N$  function but did not affect the slopes. (In Sternberg's study, one experimental session was required before this strict additivity was achieved.) Furthermore, the effect of the noise was equal for both positive and negative responses.

In the holographic system, the input noise can be assumed to increase the background noise levels, thus decreasing the effective amplitudes of the neural wavefronts. In equations 43 and 44 then, noise affects the amplitude value  $A$ , while  $N$  affects the transmission coefficients. Experimentally, noise and the number of memorized items

are additive factors, as described above; holographically, they are multiplicative. It can be concluded therefore, that the detection functions are logarithmic,<sup>6</sup> thus transforming the multiplicative relation to an additive one. Since noise decreases the amplitude A, while experimentally increasing reaction time (the increase being equal for positive and negative responses), the resulting expressions are,

$$RT^+ = t_c - k \log s_r - k \log \tau_r - k \log A \quad (45)$$

$$RT^- = t_c - k \log s_o - k \log \tau_o - k \log A \quad (46)$$

k - the detection constant

It has been pointed out that the detection of the reconstructed wavefront must precede that of the directly transmitted wavefront for a positive response to be generated. This implies, in equations 45 and 46, that for a high degree of response accuracy,

$$-k \log s_r - k \log \tau_r \ll -k \log s_o - k \log \tau_o$$

$$\text{Thus } \frac{s_o}{s_r} \ll \frac{\tau_r}{\tau_o} \quad (47)$$

Since it is unreasonable to assume that the detector sensitivities are affected by the number of items memorized, the ratio of the two sensitivities must be constant with respect to N. Experimental evidence shows that the ratio of the two transmission coefficients is also a constant. As demonstrated by Sternberg (1966) and others, the slopes of the RT functions for positive and negative response are equal; response type and the number of items memorized are thus additive factors. The difference between positive and negative response latencies is constant, independent of N:

$$RT^- - RT^+ = \text{a constant}$$

substituting from 45 and 46

$$-k \log \tau_o - k \log s_o + k \log \tau_r + k \log s_r = \text{a constant}$$



Since the ratio of the two sensitivities is also constant,

$$\frac{\tau_r}{\tau_o} = \text{a constant} \quad (48)$$

This relationship assures that equation 47 can be satisfied for any arbitrary value of N. Thus, in equations 45 and 46, strict additivity is predicted between sensitivity and the number of items memorized. This prediction has been supported experimentally in a study by Swanson and Briggs (1970) who found that variations in speed and accuracy did not interact with the form of the reaction time function. Their results justify the treatment of detector sensitivities given here.

The conclusion of a logarithmic detection functions is independently testable. In a later section, logarithmic detection is evaluated against data from simple RT tasks with variable stimulus intensity. The predictions are supported and a value for k, the detection constant, is obtained that agrees with that derived from item recognition data.

Transmission coefficients. While the transmission coefficients have already been derived from neurological principles, the experimental additivity of response type and number of items stored has allowed an independent derivation. This additivity requires (equation 48) that a constant ratio holds between the direct and the reconstruction transmission coefficients for all values of N. It has been proved (Cavanagh, 1972b; see Appendix A) that only an exponential relation between transmission coefficient and exposure will satisfy this constraint, thus supporting the neurological conclusion.

From the expressions developed in equation 41,<sup>7</sup> the transmission coefficients are, for MRM coding

$$\tau_r = \lambda e^{-\alpha N + (A^2 + B^2)} \cdot \left( I_0(2\alpha AB) \right)^{N-1} \cdot I_1(2\alpha AB) \quad (49)$$

$$\tau_o = \lambda e^{-\alpha N(A^2+B^2)} \cdot (I_o(2\alpha AB))^N \quad (50)$$

Notice that the reconstruction transmission coefficient given here is half that implied by equation 41. This takes into account the fact that two first order reconstructed wavefronts are generated,  $\underline{B}$  and its complement, that divide the available energy equally (see equation 35). It is assumed that the detector only monitors the area to which  $\underline{B}$  propagates.

For DRC coding (equation 42),

$$\tau_r = \lambda e^{-\alpha N(A^2+B^2)} \cdot (\cosh(2\alpha AB))^{N-1} \cdot \sinh(2\alpha AB) \quad (51)$$

$$\tau_o = \lambda e^{-\alpha N(A^2+B^2)} \cdot (\cosh(2\alpha AB))^N \quad (52)$$

Reaction time. Equations 45, 46 and 49 through 51 now allow explicit prediction of reaction times. For the MRM code,

$$RT^+ = t_c - k \log s_r - k \log A - k \log \left( \lambda I_1(2\alpha AB) / I_o(2\alpha AB) \right) + kN(\alpha(A^2+B^2) - \log(I_o(2\alpha AB))) \quad (53)$$

$$RT^- = t_c - k \log s_o - k \log A - k \log \lambda + kN(\alpha(A^2+B^2) - \log(I_o(2\alpha AB))) \quad (54)$$

For the DRC code,

$$RT^+ = t_c - k \log s_r - k \log A - k \log \left( \lambda \sinh(2\alpha AB) / \cosh(2\alpha AB) \right) + kN(\alpha(A^2+B^2) - \log(\cosh(2\alpha AB))) \quad (55)$$

$$RT^- = t_c - k \log s_o - k \log A - k \log \lambda + kN(\alpha(A^2+B^2) - \log(\cosh(2\alpha AB))) \quad (56)$$

These equations predict all the important features of the item recognition task data:

1. The relation between reaction time and the number of items memorized is linear for both positive and negative responses.

2. The slopes of the relations are equal for positive and negative responses.

The value of the slope parameter is, for MRM coding

$$b = k(\alpha + (A^2 + B^2) - \log(I_o(2\alpha + AB))) \quad (57)$$

and for DRC,

$$b = k(\alpha + (A^2 + B^2) - \log(\cosh(2\alpha + AB))) \quad (58)$$

3. The intercept for positive responses is less than that for negatives (equation 47). The intercept difference is, for MRM

$$\Delta = k \log((s_r |_1(2\alpha + AB)) / (s_o |_o(2\alpha + AB))) \quad (59)$$

for DRC,

$$\Delta = k \log((s_r \sinh(2\alpha + AB)) / (s_o \cosh(2\alpha + AB))) \quad (60)$$

The linearity of the relations is derived independently of the linearity of the experimental item recognition data and would have been predicted even if the experimental relation were nonlinear. The equality of positive and negative slopes results from the equal effects of noise on positive and negative responses (equations 45 and 46). Finally, the positive-negative intercept difference stems from the structure of the recognition system decision logic. Thus, the success of these predictions is in no way circular; they are based on neurological principles and aspects of the item recognition data independent of the predicted features.

Optimization. It is reasonable to assume that the brain attempts to maximize its processing capacity. Such maximization implies that the brain will operate at full STM storage capacity (this is quite likely, for example, in language processing and complex problem solving) and minimize its recognition times with this memory loading (recognition or comparison, the most basic mental operation, can be assumed to take up a significant portion of total processing time).

Short term memory storage capacity is commonly referred to as the memory span and has been measured for a variety of stimulus materials. The assumption of optimization may therefore allow the expression of storage and coding parameters in terms of memory span. Determining the total differential of detection time (Appendix A), the conditions for minimization are

$$A = B \quad (61)$$

and, for MRM coding

$$\frac{I_0(2\alpha+AB)}{I_1(2\alpha+AB)} + (N_m-1) \cdot \frac{I_1(2\alpha+AB)}{I_0(2\alpha+AB)} = N_m + \frac{I}{4\alpha+AB} \quad (62)$$

for DRC,

$$\coth(2\alpha+AB) + (N_m-1)\tanh(2\alpha+AB) = N_m - \frac{I}{4\alpha+AB} \quad (63)$$

Trial and error numerical solutions are possible for these equations so that in equations 57 and 58, the slope parameter  $b$  can be predicted given the value of the memory span for the type of material stored. The detection constant,  $k$ , in these equations is not known however. Fitting the slope parameter predictions for various values of memory span to the corresponding experimental RT slope data should therefore not only test the assumption of optimization but also estimate the value of  $k$ . The necessary data have been reported in an earlier study (Cavanagh, 1972a; see Appendix C) which compiled the results of six experiments from the memory span literature and twenty-seven experiments from the item recognition literature. In all, there were seven types of materials for which both memory spans and reaction time slopes were available with the constraint that list presentation be visual in both tasks and that test item presentation in the item recognition task also be visual.

The fit of the optimization predictions to the values from this study is shown in Figure 7. The  $r^2$  for the MRM code is .992 and that for the DRC code is .960; the estimated values of  $k$  are 137 ms and 111 ms, respectively.

-----  
 insert Figure 7

about here  
 -----

The MRM neural holographic model predicts the relation between RT slope and memory span with great accuracy. In the case of the DRC code, however, no stable minimum is possible for materials with memory spans of less than four items; its predictions for the remaining values is also not at the level of accuracy achieved by the MRM code model.

Simple reaction time with variable stimulus intensity

Analysis of item recognition data showed the function relating detection time to wavefront amplitude at the detector to be logarithmic. The stimulus intensity was assumed constant from trial to trial and the variation of transmission coefficients with  $N$  led to variations in detection time. If, conversely, transmission coefficients are held constant while stimulus intensity varies, the resulting reaction time vs. intensity relation should provide an independent test of logarithmic detection.

Creutzfeldt (1970), and others  
 Hartline and Graham (1932), have demonstrated that the output frequency of a receptor is logarithmically related to the input stimulus intensity. Since neurons have been shown to be fairly linear transducers of mean rates (Enger, Jansen, & Walloe, 1969), this logarithmic relation

between intensity and mean rate should hold at every level of neural processing. Experimental evidence supports this prediction at both the lateral geniculate (De Valois, Jacobs & Jones, 1962) and the visual cortex (Pollen, Lee, & Taylor, 1971).

Wavefront amplitude at the detector will therefore be logarithmically related to stimulus intensity. As a result, detection time should vary as a log-log function of intensity. The simple RT task, which requires subjects to respond as soon as the stimulus is detected, thus generates the data to test this prediction.

The analysis is complicated, however, by the effect of stimulus intensity on the latent period between stimulus onset and the frequency output at the receptor. Reaction time is therefore the sum of two components, this receptor or sensory latency and the detection latency. While some have argued that the sensory latency alone is responsible for reaction time variations, both Sternberg (1971) and Sanford (1970,1971) have presented evidence showing that this cannot be the case.

It may be possible to informally estimate the sensory component. The data of Hartline and Graham (1932) and that of Baker, Sanseverino, Lamarre, and Poggio (1969) show that there is a stimulus intensity beyond which only sensory latency varies while frequency remains essentially constant. At very high stimulus intensities then, reaction time will reflect the sensory component alone.

Great simplification results if a log-log relation can be assumed between the latent period at the receptor and stimulus intensity. There is no theoretical justification for such a relationship, but it does, in fact, fit the data reported for the noiseless visual receptor of the

Limulus (Hartline, 1934) reasonably well ( $r^2 = .980$ , 4 df).

With this assumption, simple RT to light for human subjects is predicted to be linearly related to the log-log value of the stimulus intensity. The slope at lower luminances reflects both the latent period and the detection time while the slope at high luminances represents the latent period alone. The detection constant,  $k$ , thus equals the difference between these two slopes.

The equations expressing this relationship are,

$$RT = c - h \cdot \log(\log I / I_0) \quad I > I_B \quad (64)$$

$$RT = c - (h + k) \cdot \{\log(\log I / I_0)\} \quad I < I_B \quad (65)$$

$h$  - slope of the sensory latency function

$k$  - detection constant

$I$  - stimulus intensity

$I_0$  - absolute intensity threshold

$I_B$  - the break intensity, above which frequency does not vary

Data for simple reaction time to light was taken from Cattell (1886), Piéron (1920), Bartlett and Macleod (1954), and Minucci and Connors (1964). The data in each study were divided into upper and lower segments by inspection. Best fitting linear relations were then determined simultaneously for the upper and lower portions of the combined data. By a liberal estimate, eighteen parameters are needed to characterize the fit: two slopes; four absolute thresholds; eight intercepts; and an additional four parameters to reflect the division of the data into upper and lower intensity segments. The model (with 12 df remaining) predicts 99.9% of the observed variance. Figure 8 illustrates the fit of the equations to the data.

-----  
 insert Figure 8

about here  
 -----

The slope at high intensities is 60.7 ms/log-log unit and accounts for 99.0% of the variance of this portion. The slope at lower intensities is 179.6 ms/log-log unit ( $r^2 = .997$ ). The value of the difference,  $k$ , between the two slopes is 119.

Figure 8 also demonstrates that there is not a clean superposition of break intensities. The slope for higher intensities might therefore be better estimated by fitting the four upper segments independently and averaging the resulting slopes. The value of  $h$  in this case is 55.3 and  $k$  is thus 124.3.

Since the assumed relation of sensory latency to intensity (i.e. log-log) has no theoretical basis and a limited empirical foundation, this analysis of simple RT must be considered informal. Nevertheless, two important features are evident. First, the logarithmic detection function is supported; second, the value of  $k$  derived from the analysis (120 to 125) is in agreement with the values determined from the optimization assumption (137 for the MRM code and 111 for DRC).  
Continuous item recognition, perceptual phenomena, and serial position

This last section deals with three miscellaneous aspects of the holographic recognition system.

First, since the system involves unbuffered transmission of information from the receptors to the detectors, it is capable of performing continuous recognition tasks without any change in its structure. Such a task has been investigated by Sternberg and Scarborough (1969); test stimuli were presented in rapid succession and the subject responded whenever one of the stimuli was a member of the list he had memorized. Reaction time was linearly related to the number of items memorized and the slope of the function did not differ from that for



the single presentation item recognition task. Continuous presentation thus appeared to have no effect on the RT function; if recognition were achieved by a serial search of memory items, the processing times involved in the task implied that these searches must be conducted in parallel. This, then, was the conclusion proposed by Sternberg and Scarborough even though there was no evidence for the time sharing overhead that would be required by such processing. In the holographic system on the other hand, stimulus wavefronts may be transmitted in a continuous stream as this is the usual processing mode of sensory events. If any wavefront represents an item that has been stored, a reconstruction is generated and its detection time follows the same function as that described in equations 53 and 55. In other words, continuous processing is the normal operation mode of the system and the single presentation item recognition task is but a special case of such processing.

Second, it was proposed at the beginning of this section on behavioural tasks that consciousness or perception accompanied the concurrent activity of the internal and external representations of a stimulus. In the item recognition task, a positive test stimulus not only elicits its external representation A, but also reconstructs its internal representation B. The classification of a positive stimulus should therefore be coincident with the perception of the stimulus. A negative test item, however, does not reconstruct its internal representation but must attempt to retrieve it from long term memory causing an additional delay before the stimulus is perceived. While the difference would be difficult to detect in the standard task, it should be readily apparent if both positive and negative stimuli are presented simultaneously. Phenomenological evidence from recognition experiments with multi-item

displays (Neisser, 1963; Briggs & Blaha, 1969; Cavanagh & Chase, 1971) support this prediction; subjects in these studies reported that positive items were "seen" or "stood out" while negative stimuli remained a blur. Evidently, no attempt was made to retrieve the internal representations of negative items, most probably because they were not essential to processing.

Finally, the holographic system predicts no serial position effects in item recognition as no decay of memory has been assumed. If decay were permitted, the linearity of the reaction time function would not be affected nor would the additivity of response types. Decay would, however, give rise to a recency effect in the serial position curve, at least for short intervals between memorization and test. Consideration of subject rehearsal strategies, perhaps emphasizing the initial items in the list (Rundus, 1970), would generate a primacy effect when expressed as position dependent inter-item storage time differences in the transmission coefficient equations. Some mix, then, of primacy and recency might allow them to cancel each other, producing no serial position effect once again. The variation in serial position effects attainable in the holographic system thus mirrors the variation found experimentally. Rehearsal protocols would, on the other hand, allow prediction of specific effects.

### Conclusions

A wide range of evidence has been given to substantiate the hypothesis of a neural holographic short term association memory. It was found that the structural coherence of the interneural connections of the brain and the linearity of neurons with respect to mean rate codes

allowed holographic storage that was in accord with neurological principles. The properties of the holographic system were analyzed for two neural codes, assuming a linear neural effect of concurrent pre- and postsynaptic impulses; mean rate modulation (MRM) appeared more reasonable in terms of operating requirements although the directional rate change code (DRC) did permit more flexibility in neural transforms.

The critical test of the hypothesis was conducted on the behavioural level where it was supported without exception on a variety of measures. Symbolic information was assumed to be represented by wavefronts of neural spike trains, thus bridging the gap between the properties of individual neurons and the characteristics of symbolic processing. A model of short term memory was developed that supported both imaging of internal information and rapid access recognition of sensory events. This model independently predicted every major feature of the item recognition RT relations including the value of the slope parameter as a function of the memory span. Here again, MRM coding found greater success than DRC.

The model was developed only to the extent necessary to test the holographic hypothesis substantively; the explicit treatment of storage, coding and retrieval parameters permits quantitative predictions of many other effects: error rates--false positives will increase with the number of items stored; inter-item similarity--generates negative acceleration in the RT function although the slope is not affected significantly; practice--the effects of practice on detection optimization and storage optimization can be differentiated; serial association--storage of the interference pattern of current input with the immediately preceding input allows temporally ordered retrieval; rehearsal--reaction

time for individual items can be predicted as a function of the number of times rehearsed; decay--determination of whether decay occurs and, if so, what form it takes, is possible. One final piece of evidence in support of holographic storage, or more accurately, of the MRM code, can be extracted from studies by Pöppel (1970) and Latour (1967). They report periodicities in simple reaction times and visual thresholds with a period in the order of 30 ms. Such results can imply mean rate<sup>modulation</sup> coding of input information with a stimulus initiated carrier frequency of about 30 Hz. It may be possible, therefore, with additional studies of this type, to directly determine the underlying neural code.

The neural holographic short term memory system proposed herein has covered the extensive range from the neuron to consciousness. It provides the structure for the comparison, storage, retrieval, and ordering operations that are the building blocks of cognitive processes. The strength of neural holographic systems derives from this ability to provide uniquely testable predictions over widely disparate levels of processing.

## References

- Baker, F. H., Sanseverino, E. R., Lamarre, Y., & Poggio, G. F. Excitatory responses of geniculate neurons of the cat. Journal of Neurophysiology, 1969, 32, 916-929.
- Bartlett N. R. & Macleod, S. Effect of flash and field luminance upon human reaction time. Journal of the Optical Society of America, 1954, 44, 306-311.
- Beurle, R. L. Properties of a mass of cells capable of regenerating pulses. Philosophical Transactions of the Royal Society of London, Series B, 1956, 240, 55-94.
- Bracey, G. W. Two operations in character recognition: A partial replication. Perception & Psychophysics, 1969, 6, 357-360.
- Briggs, G. E. & Blaha, J. Memory retrieval and central comparison times in information processing. Journal of Experimental Psychology, 1969, 79, 395-402.
- Briggs, G. E. & Swanson, J. M. Encoding, decoding, and central functions in human information processing. Journal of Experimental Psychology, 1970, 86, 296-308.
- Burrows, D. & Okada, R. Serial position effects in high-speed memory search. Perception & Psychophysics, 1971, 10, 305-308.
- Cattell, J. McK. The influence of the intensity of the stimulus on the length of the reaction time. Brain, 1886, 9, 512-515.
- Cavanagh, J. P. The relation between immediate memory span and memory search rate. Complex Information Processing Working Paper, No. 212, Carnegie-Mellon University, 1972. (a)
- Cavanagh, J. P. Two classes of holographic processes realizable in the neural realm. Paper presented at the Interdisciplinary Conference on Aspects of Cognition: Theories and Models, University of Michigan, Ann Arbor, March, 1972..(b)

- Cavanagh, J. P. & Chase, W.G. The equivalence of target and nontarget processing in visual search. Perception & Psychophysics, 1971, 9, 493-495.
- Chase, W. G. & Calfee, R. C. Modality and similarity effects in short-term memory search. Journal of Experimental Psychology, 1968, 81, 510-514.
- Clifton, C., Jr. & Birenbaum, S. Effects of serial position and delay of probe in a memory scan task. Journal of Experimental Psychology, 1970, 86, 69-76.
- Collier, R. J. & Pennington, K. S. Multicolor imaging from holograms formed on two-dimensional media. Applied Optics, 1967, 6, 1091-1095.
- Creutzfeldt, Otto D. Some principles of synaptic organization in the visual system. In Francis O. Schmitt (Ed.), The neurosciences, second study program. New York: Rockefeller University Press, 1970.
- De Valois, R. L., Jacobs, G. H., & Jones, A. E. Effects of increments and decrements of light on neural discharge rate. Science, 1962, 136, 986-988.
- Enger, P. S., Jansen, J. K. S., & Walløe, L. A biological model of the excitation of a second order sensory neurone. Kybernetik, 1969, 6, 141-145.
- Friesem, A. A. & Zelenka, J. S. Effects of film nonlinearities in holography. Applied Optics, 1967, 6, 1755-1759.
- Gabor, D. A new microscopic principle. Nature, 1948, 161, 777.
- Ginsburg, A. P. Psychological correlates of a model of the human visual system. Unpublished master's thesis, Air Force Institute of Technology, Wright-Patterson Air Force Base, Ohio, 1971.
- Griffiths, J. S. A theory of the nature of memory. Nature, 1966, 211, 1160-1163.
- Hartline, H. K. Intensity and duration in the excitation of single photoreceptor units. Journal of Cellular and Comparative Physiology, 1934, 5, 229-247.

- Hartline, H. K. & Graham, C. H. Nerve impulses from single receptors in the eye. Journal of Cellular and Comparative Physiology, 1932, 1, 277-295.
- Hebb, D. O. Organization of behavior. New York: Wiley, 1949.
- Hoving, K. L., Morin, R. E., & Konick, D. S. Recognition reaction time and size of the memory set: A developmental study. Psychonomic Science, 1970, 21, 247-248.
- Julesz, B. & Pennington, K. S. Equidistributed information mapping: An analogy to holograms and memory. Journal of the Optical Society of America, 1965, 55, 604.
- Juola, J. F. & Atkinson, R. C. Memory scanning for words versus categories. Journal of Verbal Learning and Verbal Behavior, 1971, 10, 522-527.
- Kabrisky, M., Hall, C. F., Goble, L., Gill, R. A., & Carl, J. W. Realization of a data independent pattern recognition system. Annual Symposium Record, Systems, Man, and Cybernetics, IEEE, 1971, 233-240.
- Klatzky, R. L. & Atkinson, R. C. Specialization of the cerebral hemispheres in scanning for information in short-term memory. Perception & Psychophysics, 1971, 10, 335-338.
- Kupfermann, I. & Pinsky, H. Plasticity in Aplysia neurons and some simple neuronal models of learning. In Jack T. Tapp (Ed.), Reinforcement and behavior. New York: Academic Press, 1969.
- Lashley, K. S. Brain mechanisms and intelligence. Chicago: University of Chicago Press, 1929.
- Latour, P. L. Evidence of internal clocks in the human operator. Acta Psychologica, 1967, 27, 341-348.
- Minucci, P. K. & Connors, M. M. Reaction time under three viewing conditions: binocular, dominant eye, and nondominant eye. Journal of Experimental Psychology, 1964, 67, 268-275.

- Neisser, U. Decision-time without reaction-time: Experiments in visual scanning. American Journal of Psychology, 1963, 76, 376-385.
- Perkel, D. H. & Bullock, T. H. Neural coding. Neurosciences Research Program Bulletin, 1968, 6, 221-348.
- Perkel, D. H., Schulman, J., Bullock, T. H., Moore, G. P., & Segundo, J. P. Pacemaker neurons: Effects of regularly spaced synaptic input. Science, 1964, 145, 61-63.
- Piéron, H. Nouvelles recherches sur l'analyse du temps de latence sensorielle et sur la loi qui relie ce temps à l'intensité de l'excitation. Année Psychologique, 1920, 22, 58-142.
- Pollen, D. A., Lee, J. R., & Taylor, J. H. How does the striate cortex begin the reconstruction of the visual world. Science, 1971, 173, 74-77.
- Pöppel, E. Excitability cycles in central intermittency. Psychologische Forschung, 1970, 34, 1-9.
- Pribram, K. H. Some dimensions of remembering: Steps toward a neuropsychological model of memory. In John Gaito (Ed.), Macromolecules and behavior. New York: Appleton-Century-Crofts, 1966.
- Pribram, K. H. The neurophysiology of remembering. Scientific American, 1969, 220, 73-86.
- Pribram, K. H. Languages of the brain. Englewood Cliffs, New Jersey: Prentice-Hall, 1971.
- Rundus, D. Analysis of rehearsal processes in free recall. Journal of Experimental Psychology, 1971, 89, 63-77.
- Sanford, A. J. Rating the speed of a simple reaction. Psychonomic Science, 1970, 21, 333-334.
- Sanford, A. J. Effects of changes in the intensity of white noise on simultaneity judgements and simple reaction time. Quarterly Journal of Experimental Psychology, 1971, 23, 269-303.



- Segundo, J. P., Perkel, D. H., Wyman, H., Hegstad, H., & Moore, G. P. Input-output relations in computer-simulated nerve cells. Influence of the statistical properties, strength, number, and interdependence of excitatory presynaptic terminals. Kybernetik, 1968, 4, 157-171.
- Sharpless, S. K. Reorganization of function in the nervous system-- use and disuse. In Victor E. Hall (Ed.), Annual Review of Physiology, 1964, 26, 357-388.
- Sternberg, S. High-speed scanning in human memory. Science, 1966, 153, 652-654.
- Sternberg, S. Two operations in character recognition: Some evidence from reaction-time measurements. Perception & Psychophysics, 1967, 2, 45-53.
- Sternberg, S. Decomposing mental processes with reaction-time data. Paper presented at meeting of Midwestern Psychological Association, Detroit, May, 1971.
- Sternberg, S. & Scarborough, D. L. Parallel testing of stimuli in visual search. Paper presented at the International Symposium on Visual Information Processing and Control of Motor Activity, Sofia, Bulgaria, July 1969.
- Swanson, J. M. & Briggs, G. E. Information processing as a function of speed vs. accuracy. Journal of Experimental Psychology, 1969, 81, 223-229.
- Tokarski, J. M. J. The effect on the hologram record of a nonlinear relationship between amplitude transmission and exposure. Applied Optics, 1968, 7, 989-990.
- Upatnieks, J. & Leonard, C. D. Characteristics of dielectric holograms. IBM Journal of Research and Development, 1970, 14, 527-532.
- van Heerden, P. J. Theory of optical information storage in solids.

Applied Optics, 1963, 2, 393-400.

Westlake, P. R. Towards a theory of brain functioning: The possibilities of neural holographic processes. Conference Proceedings of the 20<sup>th</sup> Annual Conference on Engineering in Medicine and Biology, IEEE, 1967.

Westlake, P. R. Towards a theory of brain functioning: A detailed investigation of the possibilities of neural holographic processes. (Doctoral dissertation, University of California, Los Angeles) Ann Arbor, Michigan: University Microfilms, 1968. No. 68-12477.

Westlake, P.:R. The possibility of neural holographic processes within the brain. Kybernetik, 1970, 7, 129-153.

Yio, J. H. & Santa, J. L. Reaction time in short-term recognition with digits and letters. Psychonomic Science, 1970, 20, 121-122.

## Footnotes

1. This research was supported in part by Public Health Service Research Grant MH-07722 from the National Institute of Mental Health.
2. I am very grateful to Dr. William Chase, John Parkman, Susan Peters, and Richard Young for various combinations of empirical, theoretical, and spiritual help and especially to Dr. Tom Calvert for invaluable assistance in developing the neurophysiological model reported here.
3. Mean rate codes are, in general, the most suitable for holographic purposes. If more than one type of code supports storage and reconstruction, it might be possible to superimpose the various codes (assuming they are orthogonal) and simultaneously store and retrieve independent information wavefronts in the same storage area. Distribution coding, although it has been frequently observed (Perkel & Bullock, 1968), is an improbable candidate for significant holographic processing. First of all, with many weak, independent synaptic inputs (which must be assumed for redundant storage to occur), the distribution of output firing bears no relation to input distributions (Segundo, Perkel, Wyman, Hegstad & Moore, 1968). Second, even under the condition of a limited number of relatively strong inputs, storage and retrieval of distribution parameters other than the mean is possible only in a number of special cases.

## Footnotes

1. This research was supported in part by Public Health Service Research Grant MH-07722 from the National Institute of Mental Health.
2. I am very grateful to Dr. William Chase, John Parkman, Susan Peters, and Richard Young for various combinations of empirical, theoretical, and spiritual help and especially to Dr. Tom Calvert for invaluable assistance in developing the neurophysiological model reported here.
3. Mean rate codes are, in general, the most suitable for holographic purposes. If more than one type of code supports storage and reconstruction, it might be possible to superimpose the various codes (assuming they are orthogonal) and simultaneously store and retrieve independent information wavefronts in the same storage area. Distribution coding, although it has been frequently observed (Perkel & Bullock, 1968), is an improbable candidate for significant holographic processing. First of all, with many weak, independent synaptic inputs (which must be assumed for redundant storage to occur), the distribution of output firing bears no relation to input distributions (Segundo, Perkel, Wyman, Hegstad & Moore, 1968). Second, even under the condition of a limited number of relatively strong inputs, storage and retrieval of distribution parameters other than the mean is possible only in a number of special cases.

4. While an arriving spike may initiate an action potential (or suppress an imminent one in the case of inhibitory input) at or near the receiving postsynaptic site, this spatio-temporal input output dependence only occurs with significant frequency for the few synapses near the axon hillock. With the number of input processes in the order of thousands (10,000 synapses is typical in the cortex), the majority of spatio-temporally simultaneous pre- and postsynaptic action potential arrivals will occur as the postsynaptic action potential sweeps through the dendritic tree. Thus, for determining the rate at which these events are achieved, the input and output processes are effectively independent.

5. A, the sensory representation, is assumed to be the end result of sensory processing, whatever the feature extractions or transformations that that may include. For example, in the visual system, A might be the output of area 19 of the visual cortex. The transforms required by the holographic system are simply those that allow separation of reconstructed images; no other properties are necessary to support storage and retrieval. Additional properties are required, however, to achieve the pattern recognition ability demonstrated by the brain. Kabrisky, Hall, Goble, Gill, and Carl (1971) and Ginsburg (1971) have analyzed the various possible neural transforms that are in accord with human pattern recognition and perceptual illusions. It is not necessary that these be the transforms that map A onto the storage field neurons, they could equally well precede the production of the A wavefront. Finally, the analysis of the holographic recognition system assumes that X, Y, W, and Z are linear transforms with respect to the average amplitude of a wavefront. This implies that the column sums of each transform must be constant and allows the input

(a and b) and output (u and v) wavefronts to be represented by the values of A, B and c at a single arbitrary neuron in the storage field. This assumption simplifies analysis but is not essential in any way for holographic storage.

6. The logarithmic detection is very significant from another viewpoint. The neural holographic system that has been described is linear in terms of mean rates; a fundamental characteristic of random (Poisson) spike trains is, however, that the variance of the spike rate is linearly related to the mean. Thus, while the amplitude description of a wavefront is invariant over different absolute levels of firing (e.g. at different base rates, which change as  $\tau$  changes during storage, or different directions of change--increase or decrease), the variance in which the amplitude information is submerged is variable. The logarithmic function is the one function that transforms the dependence of the variance on the mean to an invariance. The detectability of wavefronts is thus independent of absolute firing levels only in the case of logarithmic detection.

7. The expressions used here are thus those developed assuming constant amplitude moduli at all storage neurons. Since the detector cannot separate the true reconstruction from the distortion and noise terms arising from variable moduli, it responds to the sum of the first arriving signals. This sum is best predicted by the the expressions for constant moduli as they include all the secondary terms. The suppression of the distortion and noise may then be accomplished by reverberatory feedback after some time lag.

## Figure Captions

Fig. 1. Optical holography.

Fig. 2. Structure of the neural holographic system. Underscored variables represent the wavefronts of spike trains at various locations. Open circles are neurons, connecting lines are axons and their telodendria. The feedback loops indicate the possibility of reentrant networks.

Fig. 3. A single neuron in the storage field.  $\underline{A}$  and  $\underline{B}$  are the sums of all the input effects from  $\underline{a}$  and  $\underline{b}$ , respectively. The mean output firing rate,  $\underline{c}$ , of the cell is linearly related to the input.

Fig. 4. An holographic short term memory system. External information is represented by wavefront propagation from input ( $\underline{a}$ ) through the storage field ( $\underline{A}$ ) to the output field ( $\underline{u}$ ), internal information, by propagation from  $\underline{b}$  through  $\underline{B}$  to  $\underline{v}$ .

Fig. 5. Schematic of system activity upon presentation of a test stimulus. The gate signifies that a reconstruction will occur only if the interference pattern appropriate to the test stimulus has been stored. The inhibitory input to the direct wavefront detector permits a positive response if the reconstructed wavefront is detected before the direct wavefront.  $A$ ,  $c_r$ , and  $c_o$ , are wavefront amplitudes,  $I$  is the stimulus intensity and  $I_o$  is the absolute threshold.

Fig. 6. Typical reaction time results for the item recognition task.  $N$  is the number of items memorized.

Fig. 7. Prediction of RT slopes for various classes of stimuli. The linear relationship between the optimized slope parameter predicted from observed memory span and the observed RT slopes (data from Cavanagh, 1972a) is shown for both neural codes--the DRC code does not permit optimization for memory spans of less than four. The stimulus classes and their memory spans are indicated beside the appropriate data points. The slopes of these linear relations estimate  $k$ , the detection constant.

Fig. 8. Simple RT as a log-log function of stimulus intensity. Regressions are shown for the upper segment (high intensities) and lower segment (lower intensities) combined. The fits for the four studies have been superimposed for clarity. The difference between the upper and lower segment slopes estimates the detection constant  $k$ .



FIGURE 2

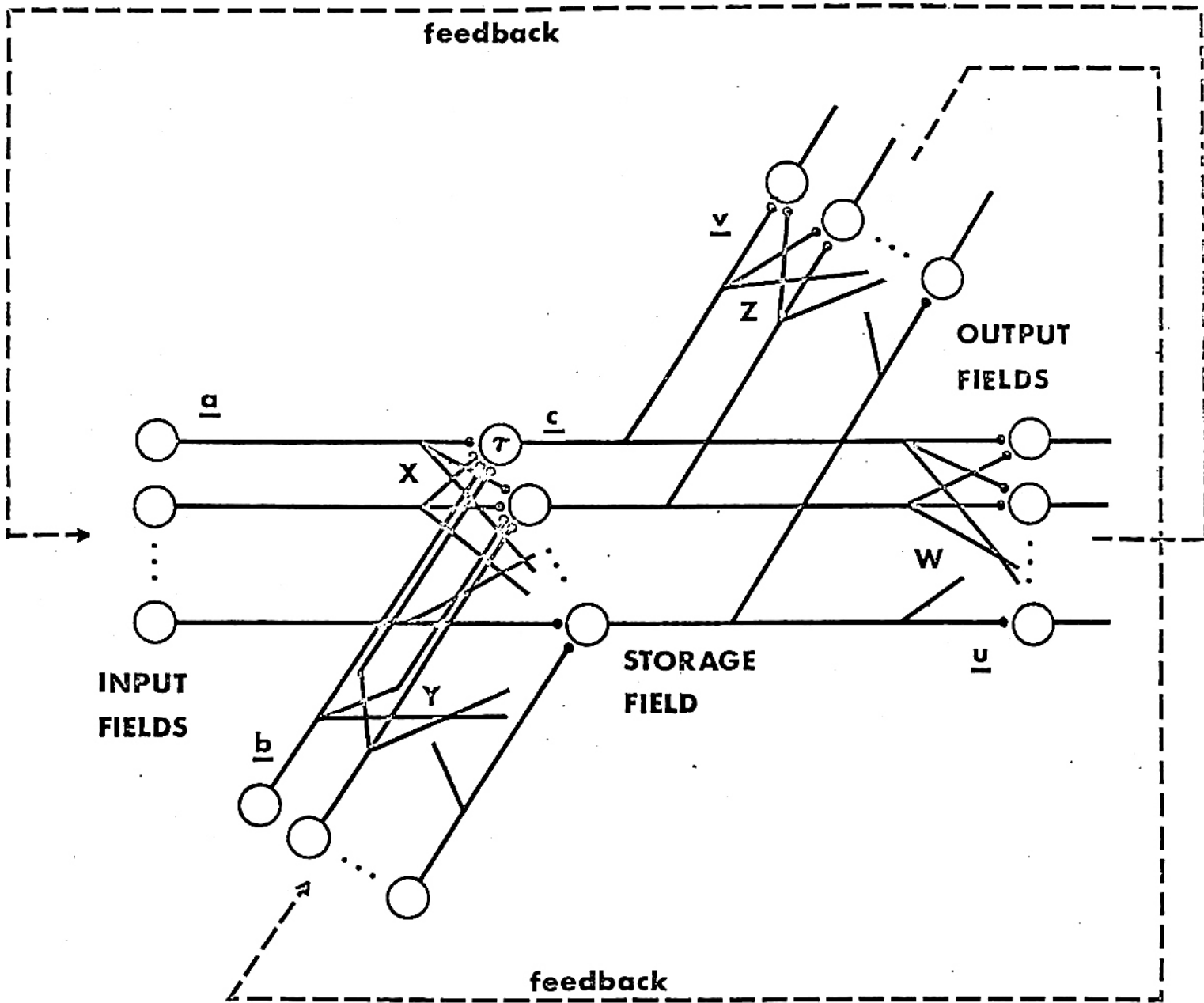
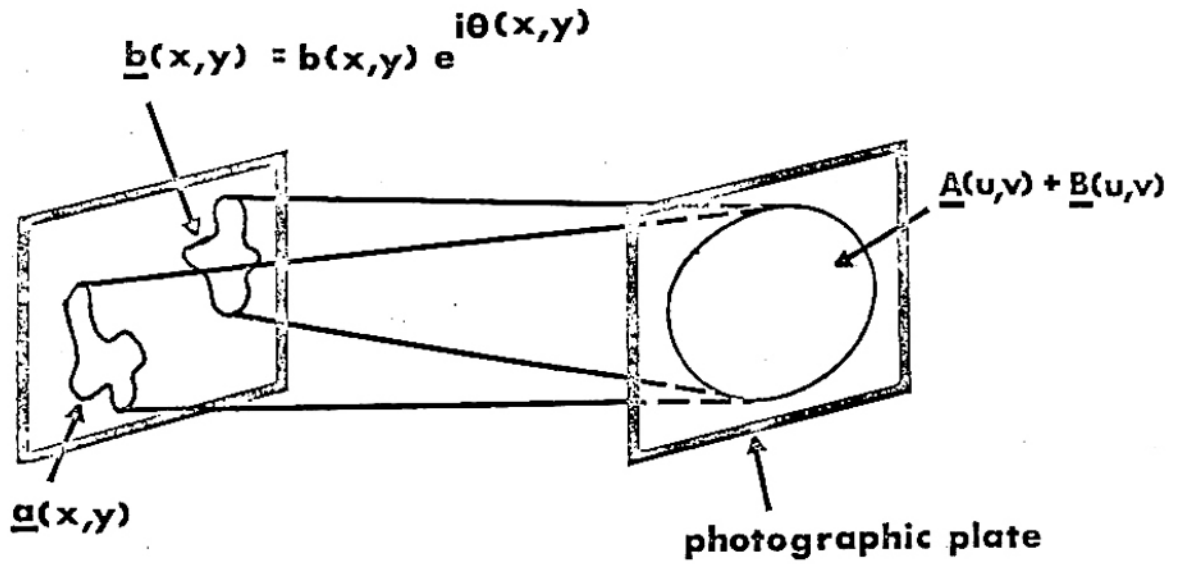


FIGURE 1

RECORDING



RECONSTRUCTION

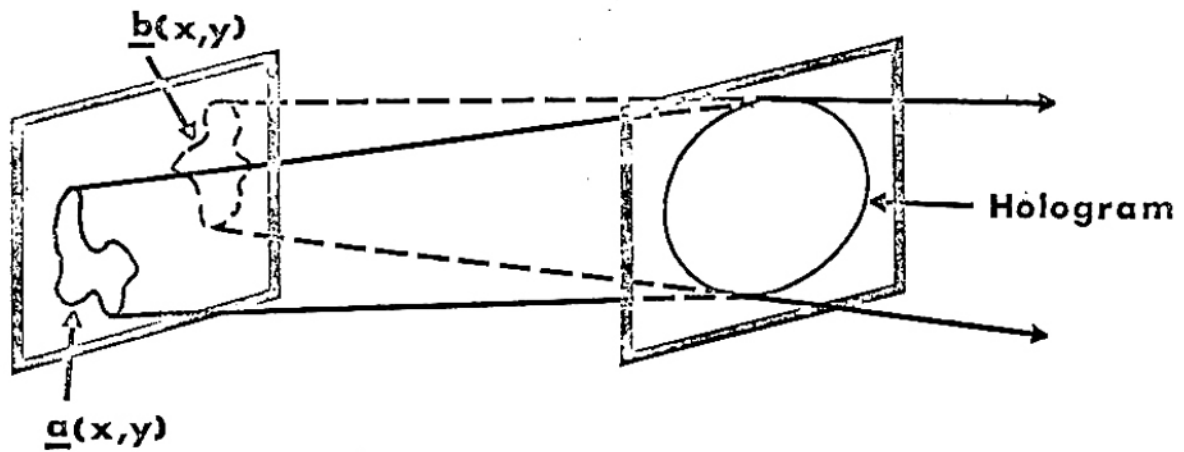
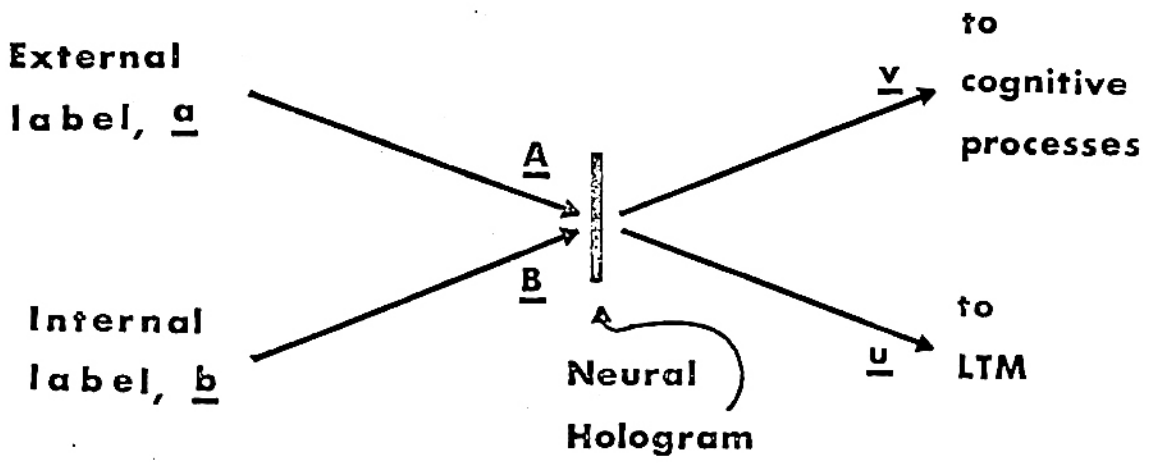
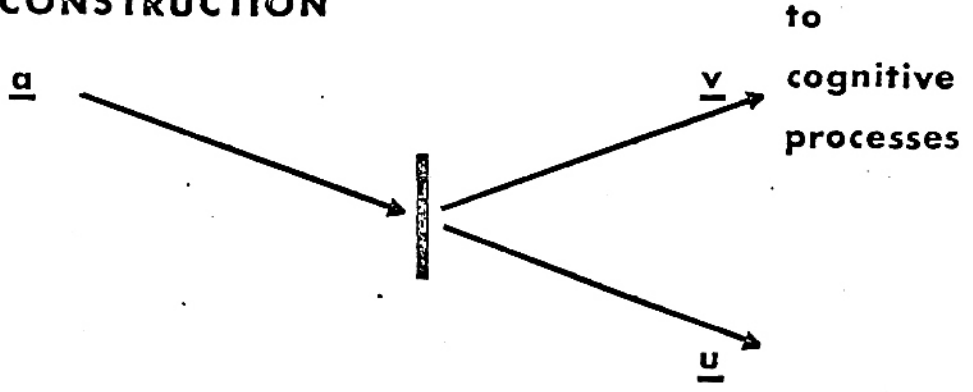


FIGURE 4

**STORAGE**



**RECONSTRUCTION**



**NO RECONSTRUCTION - a' NOT STORED**

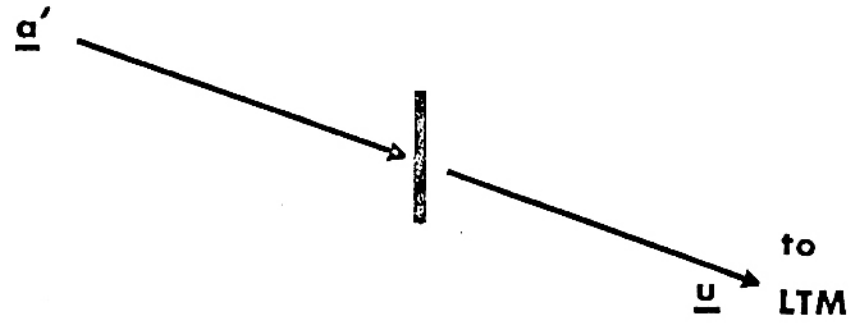


Figure 3

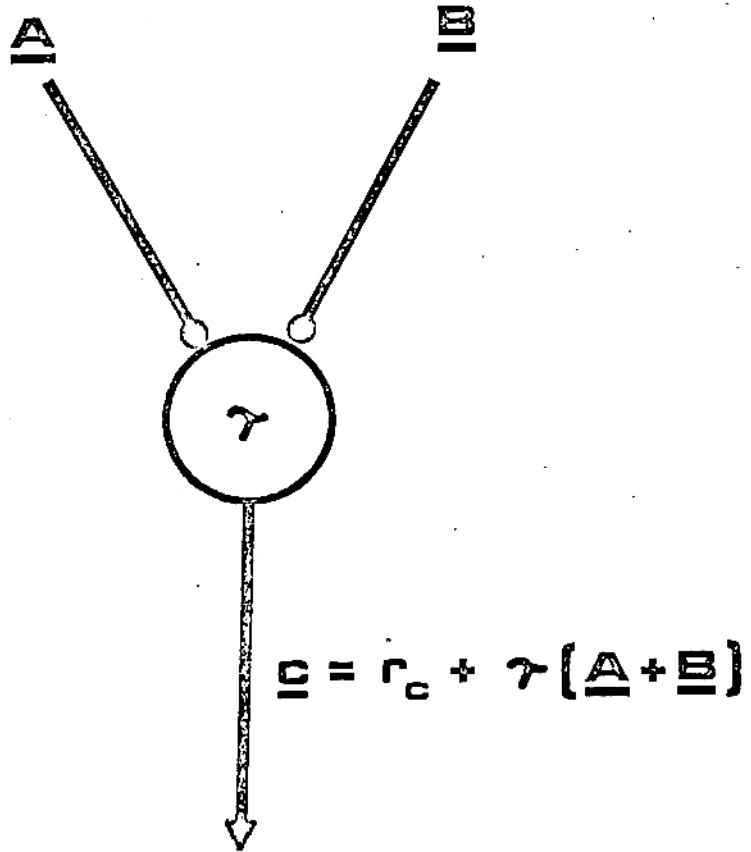


Figure 3

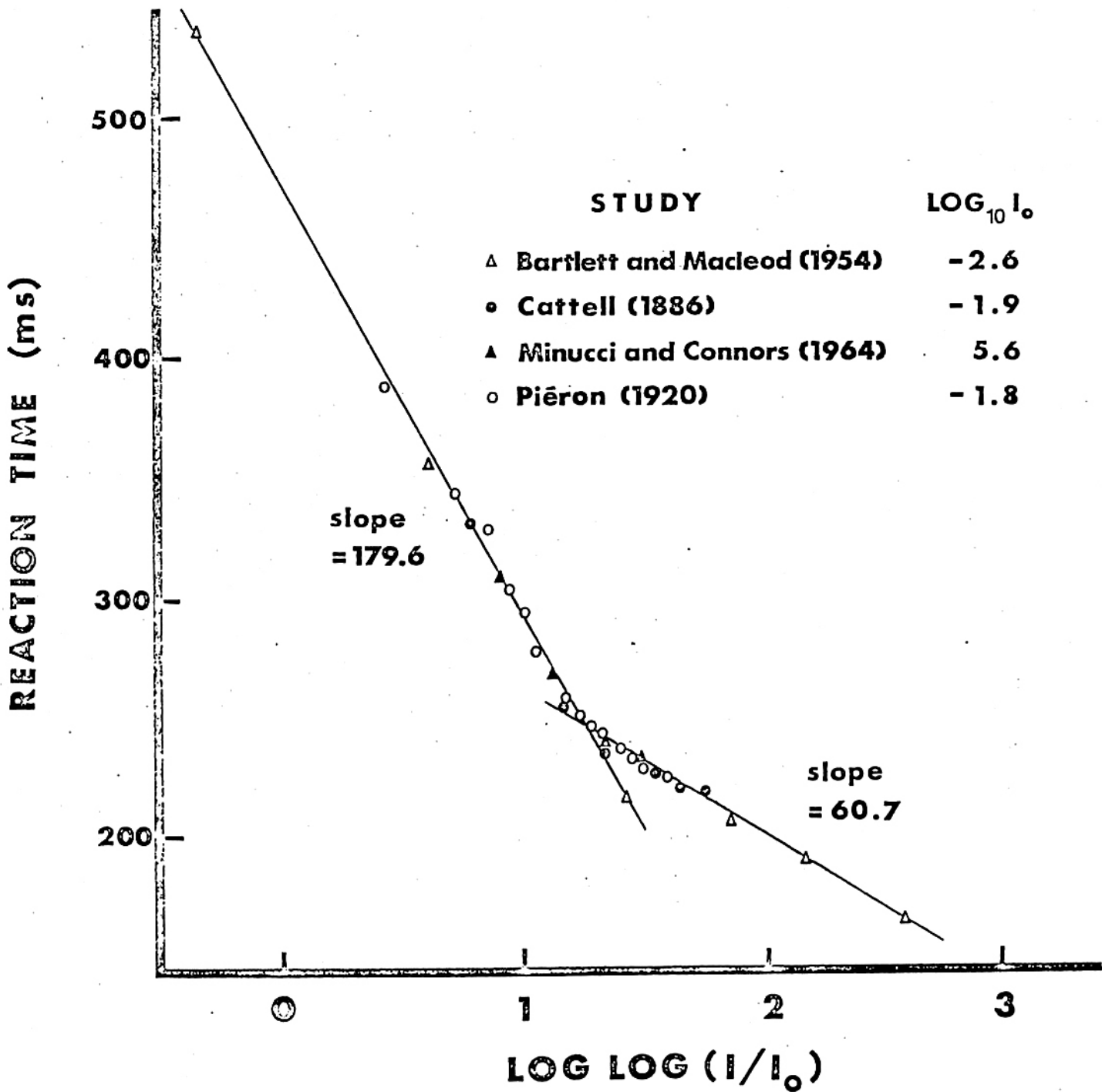
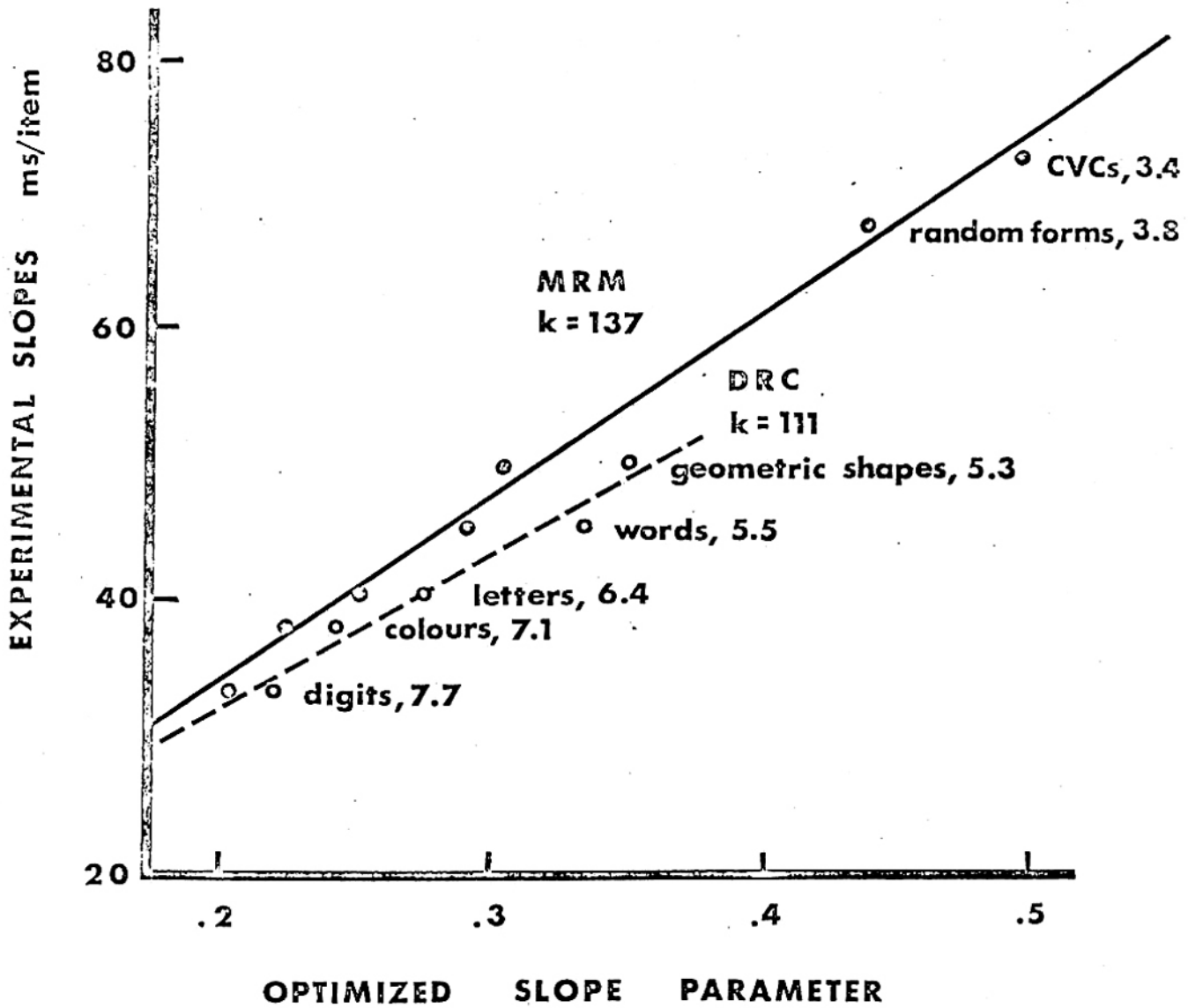


Figure 7



Appendix A: Constant ratio transmission coefficients

The transmission coefficient can be expressed as a function,  $g$ , of the sum of the  $A$  and  $B$  input over  $N$  exposures where the sum is represented by the integral over storage time of some other function,  $h$ , of  $A+B$ .

$$\tau = g\left\{\int_0^{Nt} h(A(t)+B(t)) dt\right\} \quad (1)$$

The function  $h$  can be expanded as a power series and integrated term by term.

MRM coding. Assuming, as in equation 21, that the duration of each exposure has no relation to the modulating period, the sum for each exposure is estimated from the average value over one period of modulation.

The integrals of odd powers of cosines are thus zero and those of even powers are constants. Expressing the result as a general power series,

$$\tau = g\left\{Nt(a_0 + a_2(A^2+B^2) + a_4(A^4 + 2A^3B + \frac{3}{2}A^2B^2 + 2AB^3 + B^4) + \dots) + t \cdot \sum_{j=1}^N (b_2 \cos \gamma_j + b_3 \cos^2 \gamma_j + b_4 \cos^3 \gamma_j + \dots)\right\}$$

Collapsing constant terms and terms varying with  $j$ :

$$\tau = g\left\{\Lambda + \sum_{j=1}^N \Omega_j\right\} \quad (2)$$

$\Lambda$  - constant independent of  $j$

$\Omega$  - terms varying with  $j$

The multivariate Fourier cosine series for  $\tau$  is

$$\tau = \sum_{m_1=0}^{\infty} \dots \sum_{m_N=0}^{\infty} \{T_{m_1 m_2 \dots m_N} (\cos(m_1 \gamma_1) \cos(m_2 \gamma_2) \dots \cos(m_N \gamma_N))\}$$

The direct transmission coefficient is

$$\tau_0 = T_{00\dots 0} = \frac{1}{(2\pi)^N} \int_{\gamma_1=0}^{2\pi} \dots \int_{\gamma_N=0}^{2\pi} g\left(\Lambda + \sum_{j=1}^N \Omega_j\right) d\gamma_1 \dots d\gamma_N \quad (3)$$

and the reconstruction transmission coefficient for the  $i^{\text{th}}$  wavefront is

$$\tau_{ri} = T_{0..m_i..0} = \frac{1}{2 \cdot 2^{N-1} \cdot \pi^N} \cdot \int_{\gamma_i=0}^{2\pi} \dots \int_{\gamma_N=0}^{2\pi} g(\lambda + \sum_{j=1}^N \Omega_j) \cdot \cos \gamma_i \, d\gamma_1 \dots d\gamma_N \quad (4)$$

where  $m_i=1$

and the factor of one half signifies that of the two first order reconstructions, only one is the desired B wavefront. By equation 48, the two coefficients must be linearly related.

$$\tau_0 = c \cdot \tau_r \quad (5)$$

In equations 3 and 4 above, this relationship requires that the integrals with respect to  $\gamma_i$  be linearly related independent of  $N$ .

$$\frac{d}{dN} \left\{ \int_{\gamma_i=0}^{2\pi} g(\lambda + \sum_{j=1}^N \Omega_j) \, d\gamma_i \right\} = c \frac{d}{dN} \left\{ \int_{\gamma_i=0}^{2\pi} g(\lambda + \sum_{j=1}^N \Omega_j) \cdot \cos \gamma_i \, d\gamma_i \right\} \quad (6)$$

This is only satisfied if the factors in the argument of  $g$  that vary with  $N$  are multiplicatively separable from those that vary with  $\gamma_i$ ,

$$g(\lambda + \sum_{j=1}^N \Omega_j) = h_1(\lambda + \sum_{\substack{j=1 \\ j \neq i}}^N \Omega_j) \cdot h_2(\Omega_i)$$

substituting in 6 and taking the derivative with respect to  $N$  gives

$$\frac{d(h_1(\lambda + \sum_{\substack{j=1 \\ j \neq i}}^N \Omega_j))}{dN} \cdot \int_{\gamma_i=0}^{2\pi} h_2(\Omega_i) \, d\gamma_i = c \cdot \frac{d(h_1(\lambda + \sum_{\substack{j=1 \\ j \neq i}}^N \Omega_j))}{dN} \cdot \int_{\gamma_i=0}^{2\pi} h_2(\Omega_i) \cdot \cos \gamma_i \, d\gamma_i$$

This relation is identically true for all  $N, h_1$ , and  $h_2$ . Thus, equation 7 describes the essential characteristic of the function  $g$ ; only if  $g$  is the exponential function will equation 7 be satisfied:

$$\tau = e^{\lambda + \sum_{j=1}^N \Omega_j} \quad (8)$$



DRC coding. Reconstruction can only be obtained in the DRC case if the power series contains only even powers of  $(\underline{A}+\underline{B})$  for reasons explained in the text. Expanding equation 1 of this appendix and integrating ( $\underline{A}$  and  $\underline{B}$  do not vary over the time for each exposure):

$$\tau = g\left\{ \sum_{j=1}^N (a_0 + a_2(A^2 \text{evn}^2 \theta_j + 2AB \text{evn} \theta_j \text{evn} \phi_j + B^2 \text{evn}^2 \phi_j) + a_4(A^4 \text{evn}^4 \theta_j + 4A^3 B \text{evn}^3 \theta_j \text{evn} \phi_j + 6A^2 B^2 \text{evn}^2 \theta_j \text{evn}^2 \phi_j + \dots) + \dots \right\} \quad (9)$$

but  $(\text{evn} \theta)^{2n} = 1$

$$(\text{evn} \theta)^{2n+1} = \text{evn} \theta$$

$$\text{evn} \theta \cdot \text{evn} \phi = \text{evn}(\theta - \phi) = \text{evn} \gamma$$

thus  $\tau = g\{N(a_0 + A^2 + B^2 + A^4 + 6A^2 B^2 + B^4 + \dots) + (2a_2 AB + 4a_3 A^3 B + 4a_3 AB^3 + \dots) + \sum_{j=1}^N \text{evn} \gamma_j\}$  (10)

collapsing constants,

$$\tau = g\left(\Lambda + \sum_{j=1}^N \text{evn} \gamma_j\right)$$

expanding as a Taylor series around  $\Lambda$ ,

$$\tau = g(\Lambda) + g'(\Lambda) \cdot \left(\sum_{j=1}^N \text{evn} \gamma_j\right) + \frac{g''(\Lambda)}{2!} \cdot \left(\sum_{j=1}^N \text{evn} \gamma_j\right)^2 + \dots \quad (11)$$

where the derivatives of  $g$  are with respect to the sum of the  $\text{evn}$ 's.

Since the product of two  $\text{evn}$ 's of the same argument equals one, even terms of the Taylor expansion can be grouped into a constant portion and products of  $\text{evn}$ 's with different arguments (intermodulation portion); similarly, the odd terms can be grouped into  $\text{evn} \gamma_j$ 's multiplied by constants and products of two or more  $\text{evn}$ 's for different arguments. The constant terms are given simply by the number of combinations of  $\text{evn}$ 's of the same arguments taken two at a time.

$$\tau = \sum_{n=0}^{\infty} \frac{g^{2n}(\Lambda)}{(2n)!} \psi^{2n} \binom{2n}{2} N^n + \sum_{n=0}^{\infty} \frac{g^{2n+1}(\Lambda)}{(2n+1)!} \psi^{2n+1} \binom{2n}{2} N^n \cdot \sum_{j=1}^N \text{evn} \gamma_j + \text{products of evn's with different arguments} \quad (12)$$

The first term of equation 12 is the direct transmission coefficient; the second is the reconstruction transmission coefficient. For a constant ratio relation between these two coefficients, their expansions must be linearly related term by term. This gives

$$g^{2n}(\Lambda) = c \frac{\Psi}{2^{n+1}} g^{2n+1}(\Lambda) \quad (13)$$

The solution of 13 is the exponential function:

$$\tau = e^{(\Lambda + \Psi \sum_{j=1}^N \epsilon v \gamma_j)} \quad (14)$$

Appendix B: Optimization of detection

It can be shown that the detection time has no minima with respect to the variables  $s_r$ ,  $s_o$ ,  $\lambda$ ,  $\alpha$ , and  $t$ . There are, of course, operational minima at the end points of the intervals (if closed) over which these variables may range in the brain and movement toward these end points might be under the control of attentional processes.

Detection time can be minimized with respect to A and B with storage of the maximum number of stimulus items possible (estimated by the memory span). Allowing that detection time is optimized both for the reconstruction of the B wavefront (recognition) and of the A wavefront (imaging or recognition of internal information) and that these two operations occur with equal frequency, the average detection time for A and B wavefronts can be expressed for MRM coding as follows,

$$t_{dr} = -k \left( \log \lambda s_r + \frac{\log A + \log B}{2} + \log I_1(2\alpha t AB) + (N_m - 1) \cdot \log I_0(2\alpha t AB) - N_m \alpha t (A^2 + B^2) \right) \quad (1)$$

$$\frac{dI_0(x)}{dx} = I_1(x) \quad \text{and} \quad \frac{dI_1(x)}{dx} = I_0(x) - \frac{1}{x} I_1(x)$$

$N_m$  - memory span

$$\text{thus } \frac{\partial t_{dr}}{\partial A} = \frac{1}{2A} + 2\alpha t B \left( \frac{I_0(2\alpha t AB)}{I_1(2\alpha t AB)} - \frac{1}{2\alpha t AB} \right) + 2(N_m - 1)\alpha t B \frac{I_1(2\alpha t AB)}{I_0(2\alpha t AB)} - 2N_m \alpha t A \quad (2)$$

$$\text{and } \frac{\partial t_{dr}}{\partial B} = \frac{1}{2B} + 2\alpha t A \left( \frac{I_0(2\alpha t AB)}{I_1(2\alpha t AB)} - \frac{1}{2\alpha t AB} \right) + 2(N_m - 1)\alpha t A \frac{I_1(2\alpha t AB)}{I_0(2\alpha t AB)} - 2N_m \alpha t B \quad (3)$$

setting both partial derivatives to zero and solving simultaneously gives,

$$A = B \quad (4)$$

$$\text{and } \frac{I_0(2\alpha AB)}{I_1(2\alpha AB)} + (N_m - 1) \frac{I_1(2\alpha AB)}{I_0(2\alpha AB)} = N_m + \frac{1}{4\alpha AB} \quad (5)$$

For DRC coding,

$$\begin{aligned} t_{dr} = & -k \left( \log \lambda s_r + \frac{\log A + \log B}{2} + \log \sinh(2\alpha AB) \right. \\ & \left. + (N_m - 1) \log \cosh(2\alpha AB) - N_m \alpha (A^2 + B^2) \right) \quad (6) \end{aligned}$$

Taking the partial derivatives with respect to A and B, setting both equal to zero and solving simultaneously gives,

$$A = B \quad (7)$$

$$\text{and } \coth(2\alpha AB) + (N_m - 1) \tanh(2\alpha AB) = N_m - \frac{1}{4\alpha AB} \quad (8)$$

Inserting values for memory span into equations 5 and 8 allows a solution of  $2\alpha AB$ . These values can then be substituted into equations 57 and 58 of the text to predict the slope parameter for the given value of memory span.

Appendix C: Data relating memory span to RT function slope (from Cavanagh, 1972a)

Material	Span (items)	Slope (ms/item)	Predicted MRM parameter	Predicted DRC parameter
digits	7.70	33.4	.205	.220
colours	7.10	38.0	.223	.242
letters	6.35	40.1	.251	.277
words	5.50	45.3	.292	.334
geometrical shapes	5.30	50.0	.305	.351
random forms	3.80	68.0	.439	---
nonsense syllables	3.40	73.0	.497	---

Appendix D: Latent period vs. intensity (from Hartline, 1934)

Intensity (log <sub>10</sub> units)	Latent period (in ms) at different stimulus durations				
	.1 ms	1. ms	10. ms	100. ms	1000. ms
0	676	223	100	88	77
-1		610	224	143	136
-2			632	259	249
-3				750	505
-4					---

Appendix E: Simple RT vs. intensity

All studies measured simple RT to light.

Barlett & Macleod (1954)		Minucci & Connors, cont'd	
dark adapted; foveal presentation; 575 ms flash duration; two subjects.		Intensity	RT
Intensity (log <sub>10</sub> units)	RT (ms)	8.06	269
-2.32	535	9.10	243
-1.82	355	10.18	231
-.82	216	Piéron (1920)	
.18	205	dark adapted; no set fixation; 55ms duration; one subject	
1.18	190	Intensity	RT
3.18	165	(log <sub>10</sub> units)	(ms)
		0	339
Cattell (1886)		.60	294
two subjects		.95	279
Intensity (log <sub>10</sub> units)	RT (ms)	1.20	253
0	280	1.40	244
.85	205	1.60	228
1.36	184	2.00	208
2.09	174	2.20	202
2.50	170	2.40	196
3.00	169	2.60	194
		2.95	188
Minucci & Connors (1964)		3.20	183
dark adapted; foveal, dominant eye presentation; 60 ms duration; eight subjects		3.40	180
		4.00	175
Intensity (log <sub>10</sub> units)	RT (ms)		
7.13	308		